JBC RESEARCH ARTICLE

Asialoglycoprotein receptor 1 is a novel PCSK9-independent ligand of liver LDLR cleaved by furin

Received for publication, April 8, 2021, and in revised form, August 26, 2021 Published, Papers in Press, September 8, 2021,
https://doi.org/10.1016/j.jbc.2021.101177

Delia Susan-Resiga[1,‡], Emmanuelle Girard[1,‡], Rachid Essalmani[1], Anna Roubtsova[1], Jadwiga Marcinkiewicz[1], Rabeb M. Derbali[1], Alexandra Evagelidis[1], Jae H. Byun[2], Paul F. Lebeau[2], Richard C. Austin[2], and Nabil G. Seidah[1,*]

From the [1]Laboratory of Biochemical Neuroendocrinology, Montreal Clinical Research Institute (IRCM), Affiliated to the University of Montreal, Montreal, Quebec, Canada; [2]Division of Nephrology, Department of Medicine, McMaster University, St. Joseph's Healthcare Hamilton, Hamilton, Ontario, Canada

Edited by George DeMartino

The hepatic carbohydrate-recognizing asialoglycoprotein receptor (ASGR1) mediates the endocytosis/lysosomal degradation of desialylated glycoproteins following binding to terminal galactose/N-acetylgalactosamine. Human heterozygote carriers of ASGR1 deletions exhibit ∼34% lower risk of coronary artery disease and ∼10% to 14% reduction of non-HDL cholesterol. Since the proprotein convertase PCSK9 is a major degrader of the low-density lipoprotein receptor (LDLR), we investigated the degradation and functionality of LDLR and/or PCSK9 by endogenous/overexpressed ASGR1 using Western blot and immunofluorescence in HepG2-naïve and HepG2-PCSK9-knockout cells. ASGR1, like PCSK9, targets LDLR, and both independently interact with/enhance the degradation of the receptor. This lack of cooperativity between PCSK9 and ASGR1 was confirmed in livers of wildtype (WT) and *Pcsk9*$^{-/-}$ mice. ASGR1 knockdown in HepG2-naïve cells significantly increased total (∼1.2-fold) and cell-surface (∼4-fold) LDLR protein. In HepG2-PCSK9-knockout cells, ASGR1 silencing led to ∼2-fold higher levels of LDLR protein and DiI (1,1′-dioctadecyl-3,3,3′,3′-tetramethylindocarbocyanine perchlorate)-LDL uptake associated with ∼9-fold increased cell-surface LDLR. Overexpression of WT-ASGR1/2 primarily reduced levels of immature non-O-glycosylated LDLR (∼110 kDa), whereas the triple Ala-mutant of Gln240/Trp244/Glu253 (characterized by loss of carbohydrate binding) reduced expression of the mature form of LDLR (∼150 kDa), suggesting that ASGR1 binds the LDLR in both a sugar-dependent and -independent fashion. The protease furin cleaves ASGR1 at the RKMK^{103}↓ motif into a secreted form, likely resulting in a loss of function on LDLR. Altogether, we demonstrate that LDLR is the first example of a liver-receptor ligand of ASGR1. We conclude that silencing of ASGR1 and PCSK9 may lead to higher LDL uptake by hepatocytes, thereby providing a novel approach to further reduce LDL cholesterol levels.

Elevated levels of plasma low-density lipoprotein cholesterol (LDLc) and inflammation are the leading modifiable risk factors that drive the development and progression of atherosclerosis, the underlying cause of cardiovascular disease (CVD) (1). The removal of plasma LDLc is primarily mediated by the low-density lipoprotein receptor (LDLR) located on the surface of hepatocytes. The proprotein convertase subtilisin/kexin type 9 (PCSK9) is highly expressed in the liver (2) and, upon its secretion into plasma, binds to and enhances the degradation of the LDLR in a nonenzymatic fashion (3–6), thereby increasing circulating LDLc. Unlike gain-of-function PCSK9 variants (7), loss-of-function (LOF) variants enhance LDLR levels and promote LDLc clearance (4, 8). The development of inhibitory human monoclonal antibodies against PCSK9 represents a powerful treatment strategy for the management of CVD, which has been shown to reduce the risk of cardiovascular events in clinical populations (9). Despite these hallmark studies and their utility for lipid lowering to prevent CVD, other surface proteins on hepatocytes that bind to and modulate their interaction with PCSK9 and/or LDLR as well as LDLc uptake have not been thoroughly characterized (6).

The asialoglycoprotein receptor (ASGR) (10) is a hepatocyte type II transmembrane heterodimeric glycoprotein highly conserved among mammals. It consists of two subunits, ASGR1 (major) and ASGR2 (minor), and plays a critical role in serum glycoprotein homeostasis by mediating the endocytosis and lysosomal degradation of desialylated glycoproteins with exposed terminal galactose or N-acetylgalactosamine residues (11). ASGRs are highly expressed in hepatocytes (10). Recent studies showed that heterozygous carriers of the early termination LOF del12 mutation in the ASGR1 gene (1 in 120 persons in the Icelandic study) and another early termination heterozygote LOF ASGR1 mutant (W158X) had lower plasma levels of non-HDL cholesterol than noncarriers (12). In addition, the del12 mutation was associated with a significant 34% lower risk of CVD. Comparison of plasma LDLc decrease in LOF PCSK9 R46L (–17 mg/dl; ∼30% reduction in CVD risk) with that in LOF ASGR1 del12 mutation (–11 mg/dl) illustrates that reduction in CVD risk observed in this ASGR1 mutant (∼34%) was ∼2-fold greater than would have been predicted (*i.e.*, ∼18%) from the associated modest reduction of LDLc (12). This suggests that the atheroprotective effects of ASGR1 del12 go beyond the lowering of serum LDLc.

‡ These authors contributed equally to this work.
* For correspondence: Nabil G. Seidah, seidahn@ircm.qc.ca.

Strategies aimed at inhibiting ASGR1 expression/activity are being explored as another approach to lowering plasma LDLc and CVD risk (11). Despite the importance of PCSK9 and ASGR1 in lipid lowering and reduced CVD risk, there are currently no studies to suggest that ASGR1 and PSCK9 act in concert to impact lipid metabolism and/or atherosclerosis by modulating the binding/uptake of LDLc *via* the LDLR. The purpose of the present study was to investigate the possible regulation of the LDLR by ASGR1 and the role of PCSK9 in this process.

Results

Expression of ASGR1 and ASGR2 during development and in adult mice, and in human hepatocyte cell lines

Human ASGR is composed of a major subunit (ASGR1) and a minor subunit (ASGR2) (13). Both subunits are type II, single-pass transmembrane proteins. In ASGR1, residues Gln_{240}, Trp_{244}, and Glu_{253} in the carbohydrate recognition domain (CRD) are critical for binding exposed terminal galactose or N-acetylgalactosamine residues (https://www.uniprot.org/uniprot/P07306) (Fig. 1*A*). In mouse, whole-body *in situ* hybridization histochemistry of ASGR1 and ASGR2 mRNA expression during development and in the adult revealed that both transcripts are mainly expressed in liver starting at embryonic days 17 and 15, respectively, and showed that their expression increases until adulthood (Fig. 1*B*). A Tabula Muris compendium of single-cell RNA-Seq transcriptome data from 20 mouse organs and tissues (czbiohub.org) (14) revealed that ASGR1 transcripts are exclusively expressed in liver, specifically in hepatocytes (Fig. 1*C*). We next estimated the relative mRNA expression of ASGR1 and ASGR2 by quantitative RT-PCR in adult mouse liver and in human hepatocyte HepG2, HepG2-PCSK9-KO cells (lacking endogenous PCSK9) (15), and in the immortalized human primary hepatocytes IHH cell line (Fig. 1*D*) (15). In most cases the mRNA levels of ASGR1 were higher than those of ASGR2, especially in mouse liver.

PCSK9 reduces LDLR but not ASGR1 levels

Immunofluorescence (IF) staining of endogenous ASGR1 in HepG2-PCSK9-KO cells confirmed its presence at the

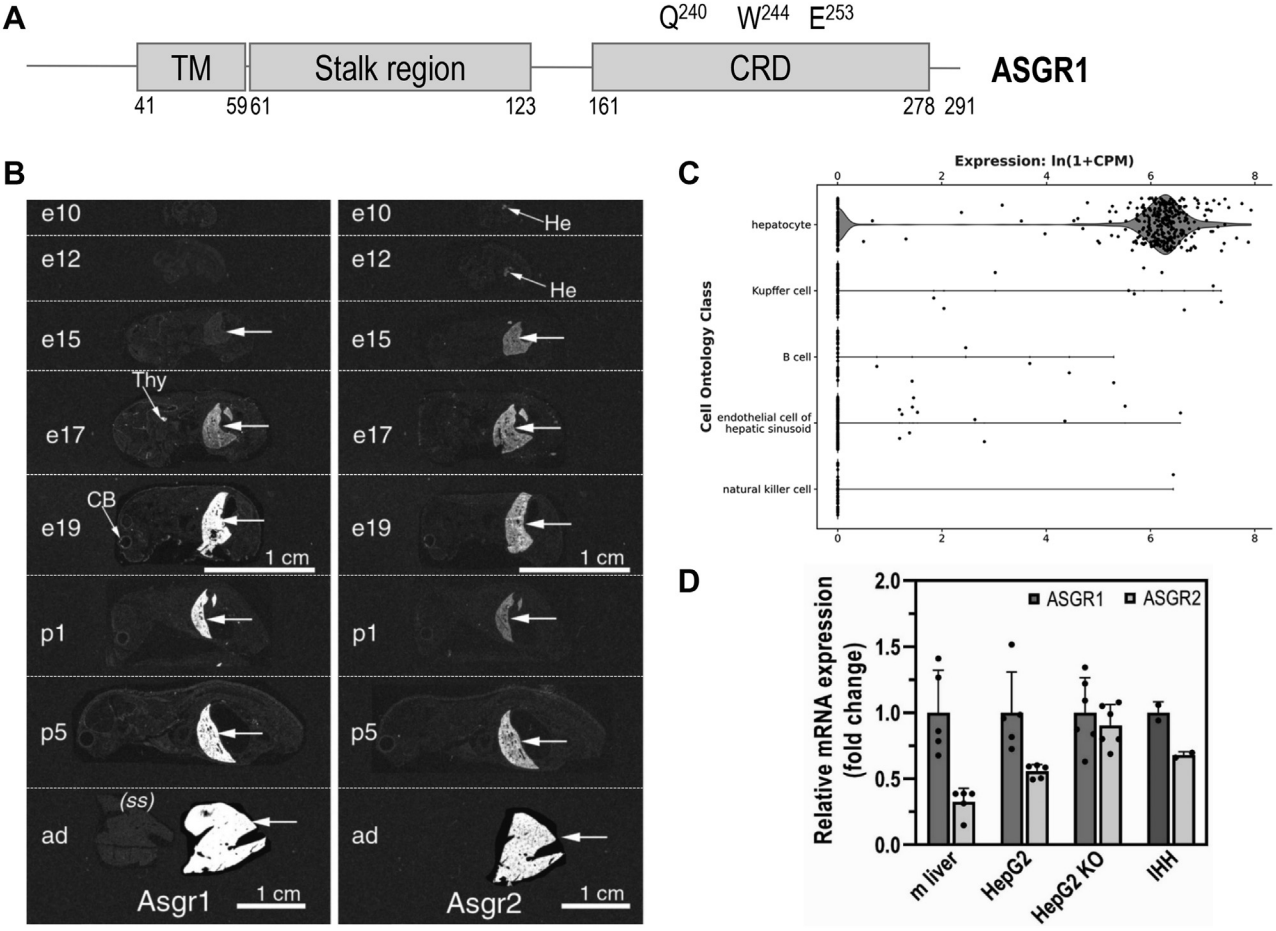

Figure 1. Expression of ASGR1 and ASGR2 in mice and cell lines. *A*, schematic representation of ASGR1, depicting its cytoplasmic N terminus (40 aa), the single transmembrane domain (TM) and its exoplasmic C terminus (~230 aa) that is composed of a stalk region and a C-terminal carbohydrate recognition domain (CRD) with three reported residues important for carbohydrate binding. *B*, *in situ* hybridization of ASGR1 and ASGR2 in mice before and after birth. *C*, a Tabula Muris Consortium of mouse liver single-cell transcriptomics by RNA Seq (czbiohub.org) emphasizes the expression of ASGR1 transcripts in hepatocytes. *D*, quantitative RT-PCR of ASGR1 and ASGR2 in mouse (m) liver, HepG2-naïve, HepG2-PCSK9-KO, and IHH cells. For each sample analyzed, the ASGR2 mRNA expression was normalized to the one of ASGR1. Quantifications are averages ±SD. ad, adult; CB, cerebellum; CPM, counts per million reads mapped; e, embryonic day; He, hepatocyte (liver); p, postnatal day; (ss), sense (negative control) cRNA probe; Thy, thymus.

plasma membrane and revealed its colocalization with the LDLR (−PCSK9; Fig. 2*A*). Circulating PCSK9 is responsible for most of its activity to reduce the levels of cell-surface LDLR in hepatocytes (6). Hence, we addressed the potential regulation of ASGR1 by exogenous purified recombinant PCSK9 (16). We thus compared the known ability of *exogenous* PCSK9 to enhance the degradation of LDLR to its effect on ASGR1 in HepG2 cells by IF (Fig. 2*A*) and Western blot (WB; Fig. 2*B*). As expected, PCSK9 reduced the endogenous levels of cell-surface LDLR (−90% by IF) and total LDLR (−40% by WB). In contrast, PCSK9 did not alter the levels of endogenous ASGR1 in both assays. Note the presence of two bands for endogenous ASGR1 (Fig. 2*B*), likely representing a major mature form (∼48 kDa) that excited the endoplasmic reticulum (ER) and a minor ER-localized immature form (∼42 kDa), as observed in other proteins (16, 17).

The effect of *endogenous* PCSK9 on LDLR and ASGR1 in HepG2 cells was next investigated following its mRNA knockdown (KD) using a smart pool of four siRNAs. This resulted in ∼70% reduction in PCSK9 mRNA and protein levels (Fig. 2, *C* and *D*). As expected (18, 19), lack of PCSK9 did not affect the mRNA levels of LDLR. In addition, no effect was observed on the mRNA levels of ASGR1, ASGR2, and the transcription factor SREBP2 implicated in PCSK9 mRNA regulation (20) (Fig. 2*C*). At the protein level, PCSK9 KD resulted in ∼1.5-fold increase in LDLR, with no change in ASGR1 (Fig. 2*D*). We conclude that, in HepG2 cells, *endogenous* and *exogenous* PCSK9 do not affect ASGR1 mRNA and/or protein levels.

To address the effect of PCSK9 on ASGR1 *in vivo*, we analyzed the levels of ASGR1 in *Pcsk9*-knockout (KO) mice (18), by liver immunohistochemistry (IHC) under non-permeable conditions (21) (Fig. 3*A*) and WB (Fig. 3*B*). The data showed that, although LDLR protein levels at the cell surface of hepatocytes (IHC) and in whole tissue (WB) were increased in *Pcsk9*-KO livers, in accordance with (21), those of ASGR1 were not affected. Overall, we conclude that, like in

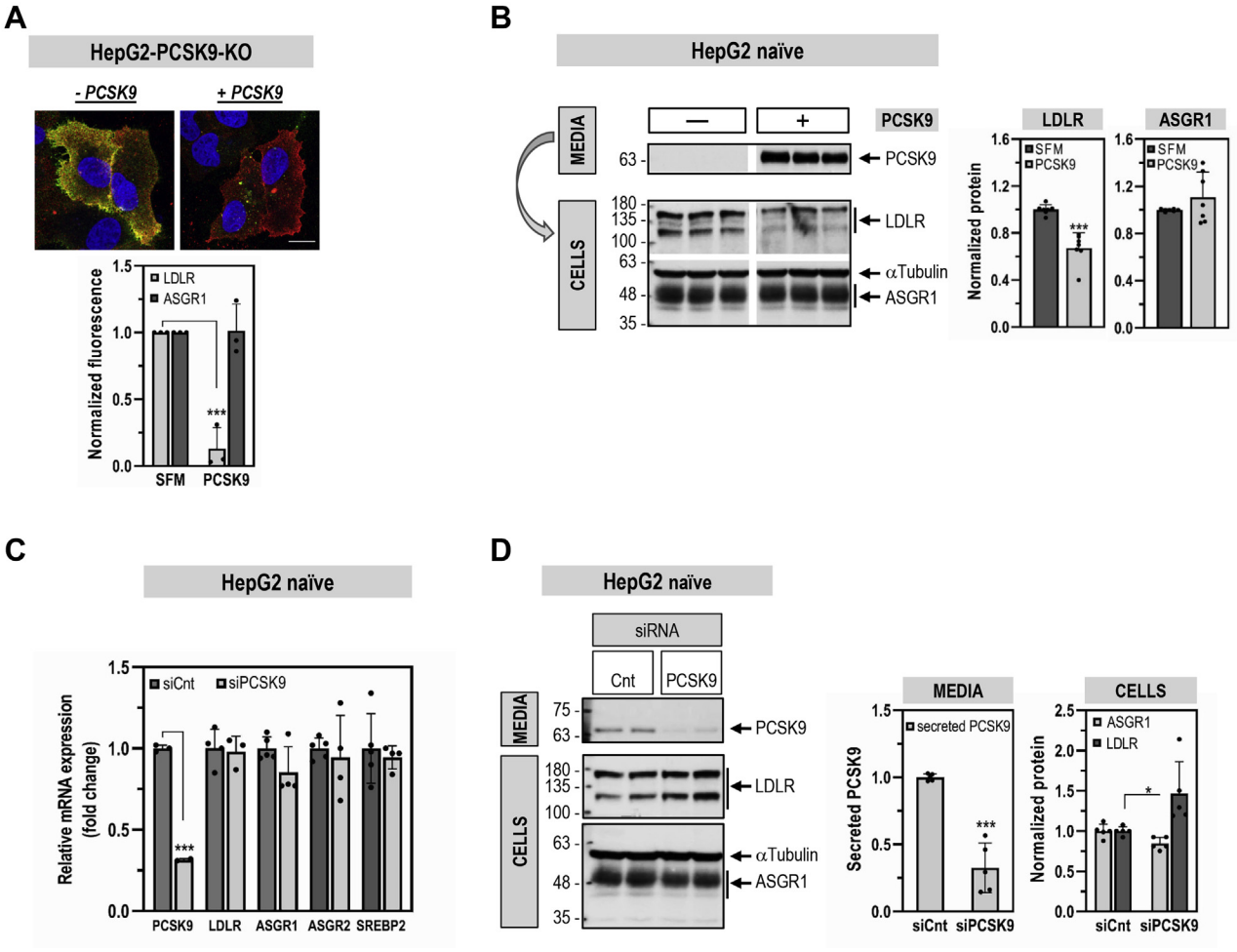

Figure 2. Comparative effects of PSCK9 on cellular LDLR and ASGR1 levels. HepG2-PCSK9-KO cells (*A*) or HepG2-naïve cells (*B*) were incubated for 20 h with media only (−PCSK9; SFM) or media containing purified PCSK9 (3 μg/ml) (+PCSK9). *A*, immunofluorescence microscopy of plasma membrane LDLR (*green signal*) and ASGR1 (*red signal*). The colocalization appears as *yellow*. The scale bar represents 15 μm. *B*, Western blot analysis of cellular LDLR and ASGR1 expression and of PCSK9 in the media of HepG2-naïve cells transfected with 20 nM nontargeting siRNA (siCnt). *C* and *D*, HepG2-naïve cells were transfected with nontargeting siRNA (siCnt) or siRNA PCSK9 (siPCSK9) at final concentrations of 10 nM and analyzed 48 h post transfection. *C*, quantitative RT-PCR analysis. *D*, Western blot analysis of cellular LDLR and ASGR1 and of secreted PCSK9. Data are representative of at least three independent experiments. Quantifications are averages ±SD. $*p < 0.05$; $***p < 0.001$ (*t* test).

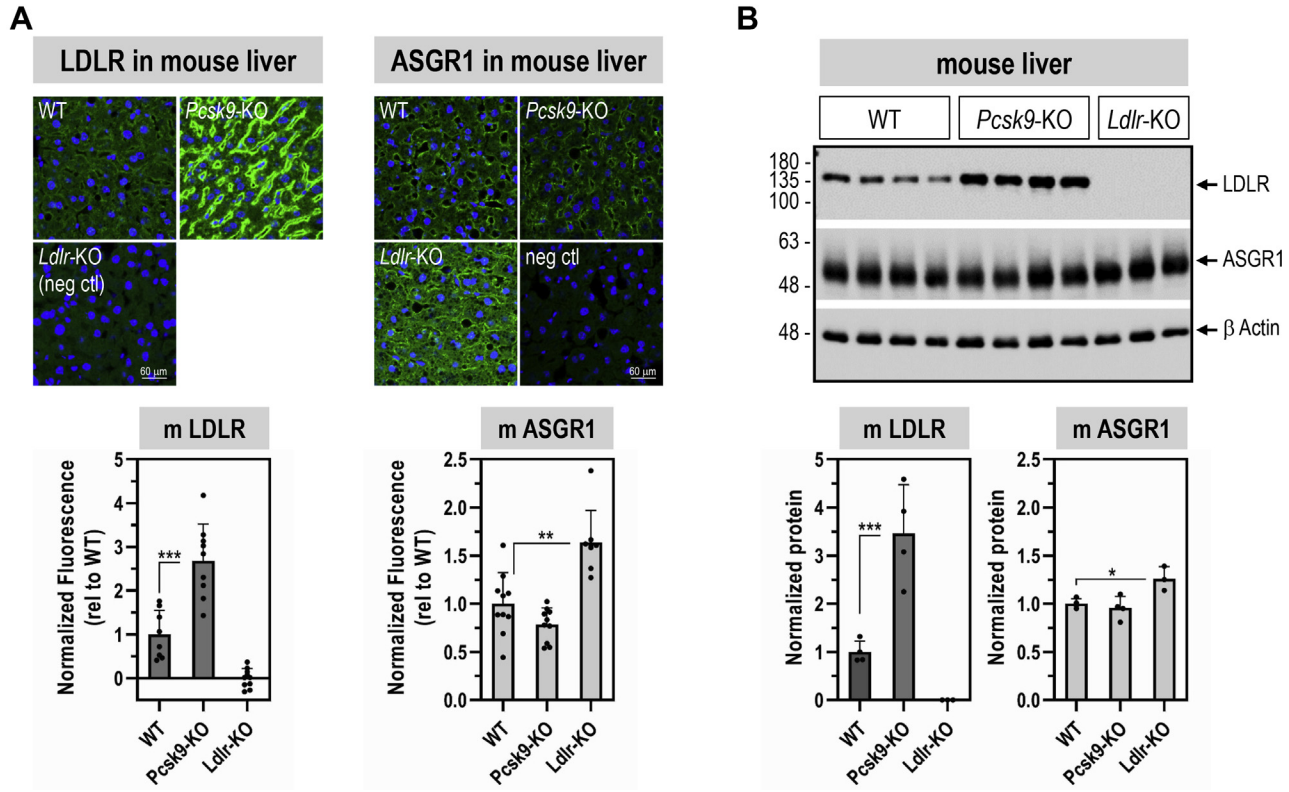

Figure 3. LDLR and ASGR1 expression levels in livers from wildtype (WT) mice and mice lacking mPCSK9 (*PCSK9*-KO) or mLDLR (*Ldlr*-KO), respectively. *A*, LDLR and ASGR1 staining by immunohistochemistry (*green signal*) in mouse liver sections. *B*, Western blot analysis of total ASGR1 and LDLR proteins in mouse livers. Data are representative of 9 to 10 mice (*A*) and 3 to 4 mice (*B*), and quantifications are averages ±SD. $^{*}p < 0.05$; $^{**}p < 0.01$; $^{***}p < 0.001$ (*t* test).

HepG2 cells, *in vivo* endogenous PCSK9 does not affect the levels of ASGR1 in mouse hepatocytes.

To analyze the impact of the lack of LDLR on ASGR1 protein, we now show that, in the liver of *Ldlr*-KO mice, both ASGR1 cell-surface immunoreactivity (Fig. 3*A*) and total ASGR1 protein by WB (Fig. 3*B*) were significantly increased by ∼1.6- and ∼1.3-fold, respectively. This suggests that ASGR1 levels could be regulated by those of the LDLR, as are circulating PCSK9 levels (6).

ASGR1 regulates LDLR levels and functionality independently of PCSK9

To examine the impact of ASGR1 on the LDLR, KD of ASGR1 (−75%) was performed in naïve HepG2 and HepG2-PCSK9-KO cells (Figs. 4 and 5). We first demonstrated that KD of ASGR1 in naïve HepG2 cells did not affect the levels of intracellular and secreted PCSK9 (Fig. 4). In contrast, ASGR1 KD resulted in a significant increase in total (WB) and cell-surface (IF) LDLR in both cell lines. Specifically, we estimated a total LDLR increase of ∼1.3-fold (Fig. 5*A*) and ∼2-fold (Fig. 5*B*) in each cell line, respectively. The corresponding cell-surface increase in LDLR was at least ∼4-fold in naïve HepG2 cells (Fig. 5, *C* and *D*) and ∼9-fold in HepG2-PCSK9-KO cells (Fig. 5*E*). Transcript analysis by quantitative RT-PCR revealed that KD of ASGR1 in HepG2 cells did not modify the mRNA levels of LDLR and SREBP2 (Fig. 5*F*). This suggests that endogenous ASGR1 reduces the total levels of LDLR protein, especially those at the cell surface, leading to the hypothesis that LDLR is a target of ASGR1, independent of PCSK9.

We next investigated whether ASGR1 affects the ability of PCSK9 to enhance the degradation of the LDLR. In both cell lines KD of ASGR1 had no significant impact on the activity of exogenous PCSK9 on the LDLR (Fig. 5, *A*–*C*). Thus, we can conclude that independently PCSK9 and ASGR1 can reduce the levels of LDLR protein.

To probe the functionality of the LDLR upon KD of ASGR1, we incubated naïve HepG2 (Fig. 5*D*) and HepG2-PCSK9-KO cells (Fig. 5*E*) with fluorescent DiI-LDL and estimated its uptake by IF. The data show that the KD of ASGR1 resulted in at least an ∼2-fold increase in DiI-LDL uptake mirroring the increase in LDLR protein levels. Thus, endogenous ASGR1 negatively regulates protein levels of LDLR and its functionality independently of PCSK9.

Since ASGR1 can act as a homodimer or heterodimer with ASGR2 (10), we next examined the effect of overexpression of ASGR1/2 in HepG2-PCSK9-KO cells. Coexpression of ASGR1 and ASGR2 at a 1:1 ratio resulted in a significant decrease in the total levels of both endogenous (−30%) and overexpressed (−55%) LDLR (WB; Fig. 6*A*). Similarly, overexpressed ASGR1/2 reduced the levels of endogenous and

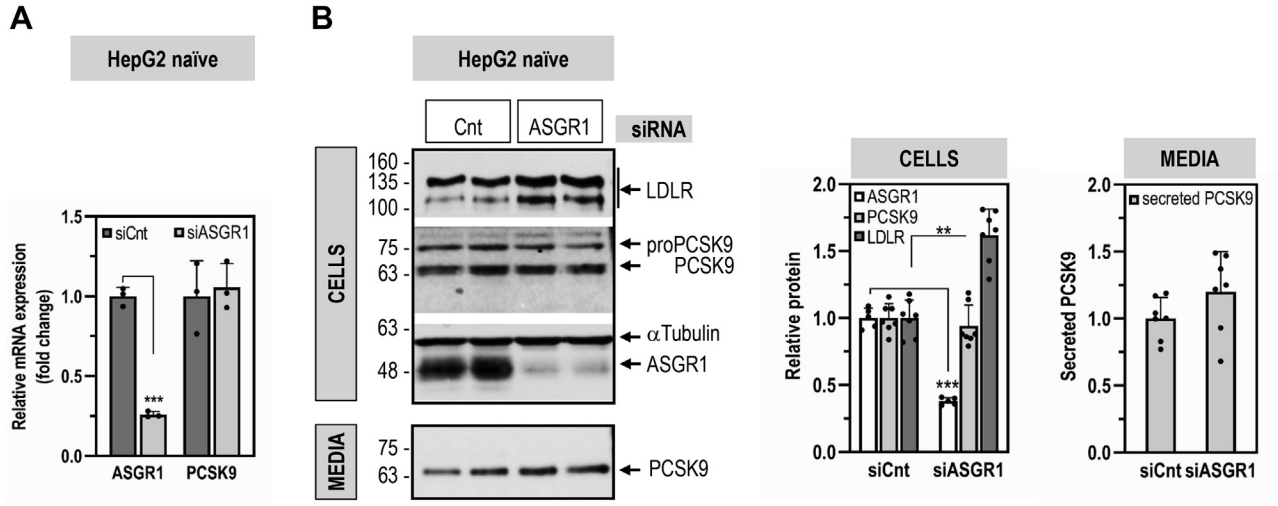

Figure 4. ASGR1 does not affect PCSK9 expression and secretion. HepG2-naïve cells were transfected for 48 h with nontargeting siRNA (siCnt) or siRNA ASGR1 (siASGR1) at final concentrations of 20 nM and analyzed by quantitative RT-PCR (*A*), or Western blot for cellular LDLR, PCSK9, and ASGR1 and for secreted PCSK9 (*B*). Data are representative of at least three independent experiments. Quantifications are averages ±SD. $^{**}p < 0.01$; $^{***}p < 0.001$ (*t* test).

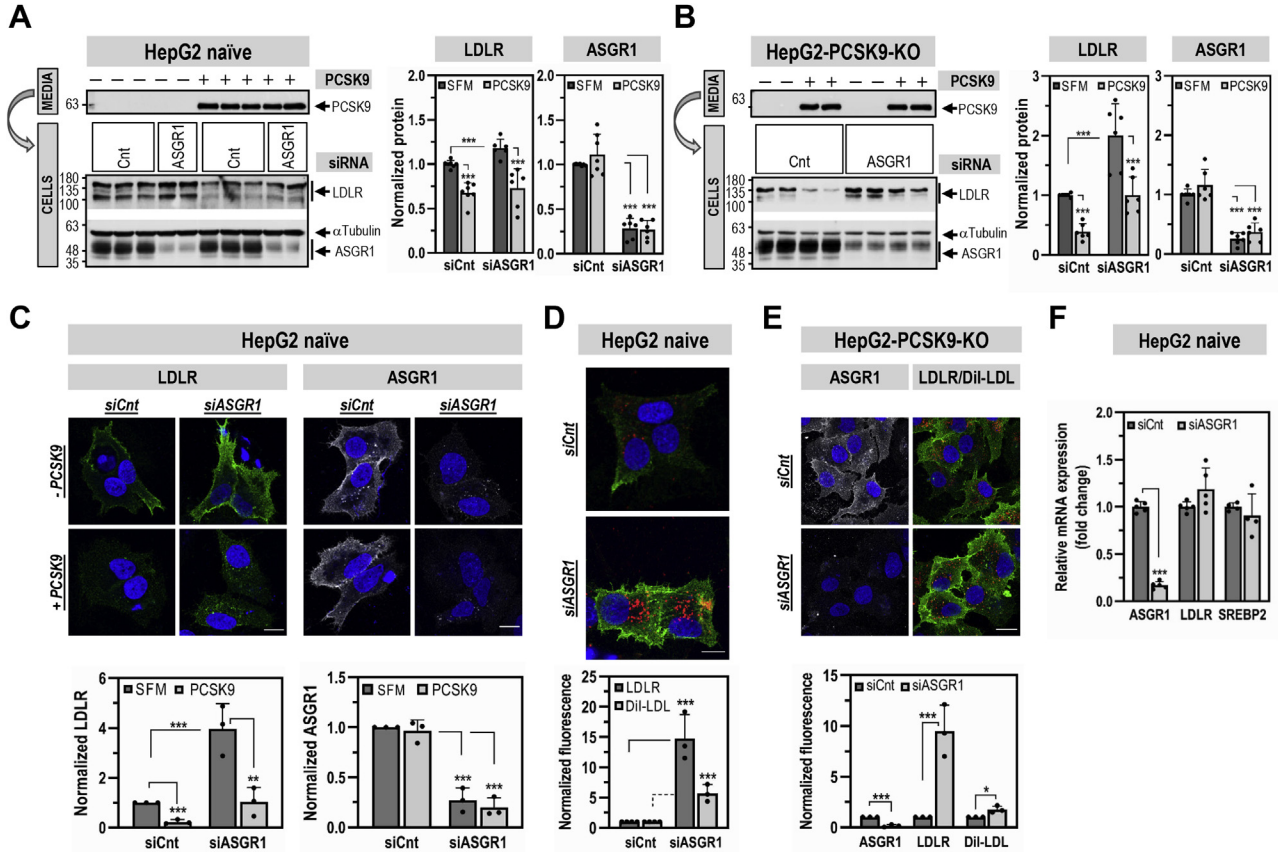

Figure 5. ASGR1 regulates LDLR levels and functionality independently of PCSK9. HepG2-naïve cells (*A*, *C* and *D*) or HepG2-PCSK9-KO cells (*B* and *E*) were transfected for 48 h with nontargeting siRNA (siCnt) or siRNA ASGR1 (siASGR1) at final concentrations of 20 nM. Cells were then incubated for the last 20 h with media only (−PCSK9; SFM) or media containing purified PCSK9 (3 μg/ml) (+PCSK9) (*A*–*C*). *A* and *B*, total protein levels of LDLR and ASGR1 were assessed by Western blot. In (*A*) the Western blot of the siCnt condition was reused from Figure 2*B*. *C*, immunofluorescence microscopy of LDLR (*green signal*) and ASGR1 (*white signal*) at the plasma membrane. *D* and *E*, immunofluorescence microscopy of plasma membrane LDLR (*green signal*) and (*E*) plasma membrane ASGR1 (*white signal*). LDLR functionality was assessed by DiI-LDL (5 μg/ml) internalization for 2 h at 37 °C before fixation (*red signal*). The scale bar represents 15 μm. *F*, quantitative RT-PCR analysis was performed on HepG2-naïve cells transfected for 48 h with nontargeting siRNA (siCnt) or siRNA ASGR1 (siASGR1) at final concentrations of 20 nM. Data are representative of at least three independent experiments. Quantifications are averages ±SD. $^{*}p < 0.05$; $^{**}p < 0.01$; $^{***}p < 0.001$ (*t* test).

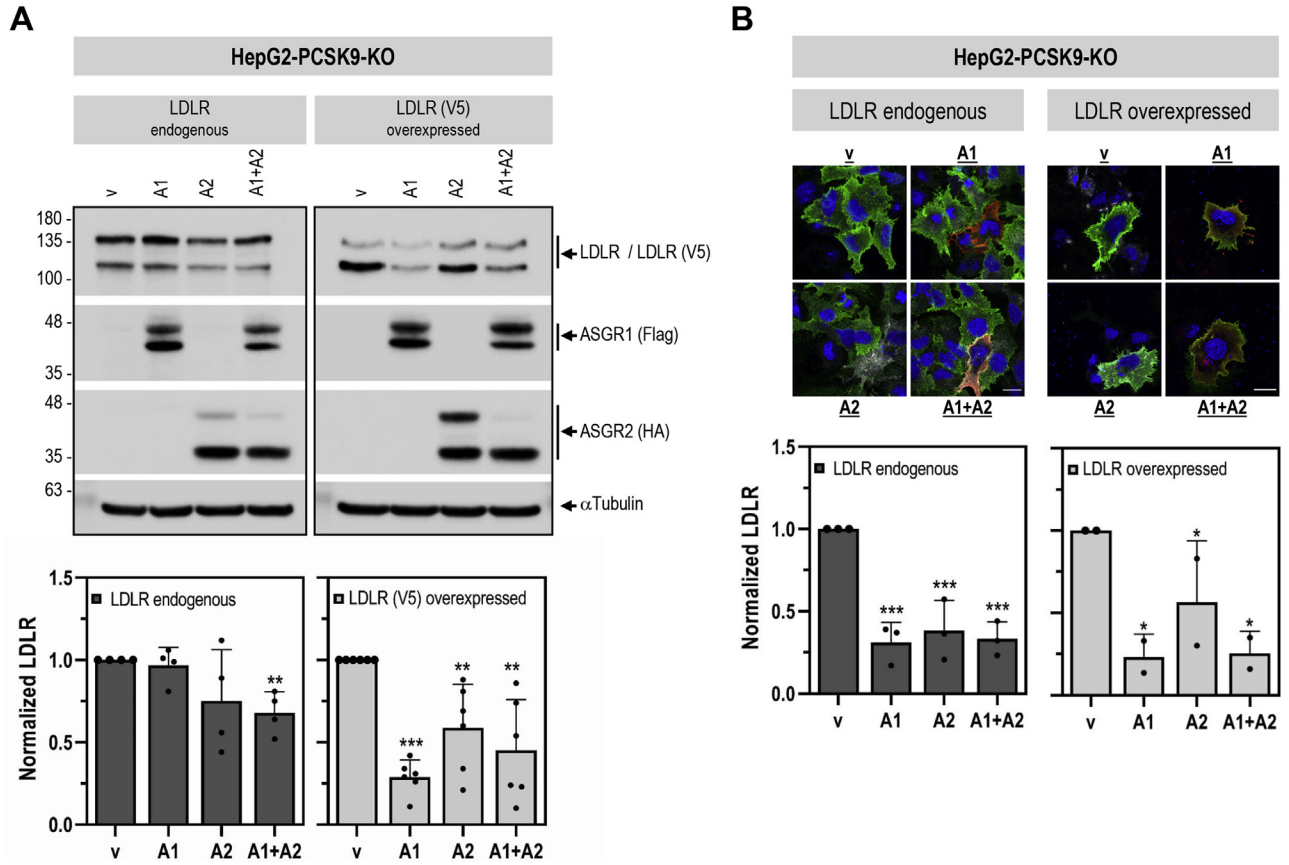

Figure 6. Overexpressed ASGR1 and ASGR2 reduce LDLR levels independently of PCSK9. HepG2-PCSK9-KO cells were transfected with Flag-tagged ASGR1 (A1), HA-tagged ASGR2 (A2), or their combination (A1 + A2) or control empty vector (V), alone or in combination with LDLR (V5). *A*, Western blot analyses and quantification of cellular LDLR (LDLR endogenous, LDLR antibody; LDLR (V5) overexpressed, V5 antibody), ASGR1 (Flag-HRP), and ASGR2 (HA-HRP). *B*, immunofluorescence microscopy of endogenous or overexpressed cell-surface LDLR (*green signal*). Quantification was performed only in cells transfected with ASGR1 (*red signal*) and/or ASGR2 (*white signal*). The scale bar represents 15 μm. Data are representative of at least two independent experiments. Quantifications are averages ±SD. $*p < 0.1$; $**p < 0.01$; $***p < 0.001$ (*t* test) are relative to the control vector condition.

overexpressed cell-surface LDLR (−75%) (IF; Fig. 6*B*). Of note, HepG2-PCSK9-KO cells endogenously express ASGR1 and ASGR2 (Fig. 1*D*). Thus, their individual overexpression would be expected to result in homodimers and/or heterodimers with the endogenous ASGRs, consequently affecting LDLR levels. This was evident in IF experiments where analyses were focused on transfected cells only (Fig. 6*B*) and in WB analyses with mAb-V5 of overexpressed LDLR-V5 (Fig. 6*A*; right panel). In all the above, overexpression of ASGR1, ASGR2, or their combination gave similar results. Altogether, KD and overexpression analyses in HepG2-PCSK9-KO cells demonstrated that, independent of PCSK9, ASGR1 negatively regulates LDLR levels and its functionality.

To dissect the ASGR1-induced degradation of the LDLR in the presence or absence of ASGR2, we selected HEK293 cells that do not express ASGR1/2 endogenously. The data showed that overexpression of ASGR1 or ASGR2 alone or together (at a 1:1 ratio) led to the same ∼30% decrease in total LDLR-V5 levels (Fig. 7). These results suggest that, under overexpression conditions, both ASGR1 and ASGR2 can degrade the LDLR, likely as homo- or hetero-oligomers (10). Hence, to maintain closer to *in vivo* conditions where both ASGR1/2 are present, we chose to use coexpressed ASGR1/2 in all subsequent experiments.

ASGR1 can bind LDLR and enhance its degradation by carbohydrate-dependent and -independent mechanisms

Coimmunoprecipitation (co-IP) analyses were used to probe the possible interaction between endogenous ASGR1 and LDLR in HepG2-PCSK9-KO cells (Fig. 8*A*). Thus, immunoprecipitation of cell lysates under nondenaturing conditions with an ASGR1 antibody, followed by separation of the immune complex by SDS-PAGE and WB, revealed that human ASGR1 coimmunoprecipitated with endogenous LDLR (mostly present as mature ∼150 kDa mLDLR) but not with CD36 or insulin receptor (IR, detected with an antibody to the β-subunit), two other endogenous membrane-bound N-glycosylated proteins (Fig. 8*A*). This suggests that endogenous ASGR1 and LDLR interact in a specific manner and form a complex independent of PCSK9. This observation was also confirmed *in vivo*, in mouse liver from wildtype (WT) and *Pcsk9*-KO mice (Fig. 8*B*).

ASGR1 is a lectin-binding protein, and Gln_{240}, Trp_{244}, and Glu_{253} in its CRD are critical for carbohydrate binding.

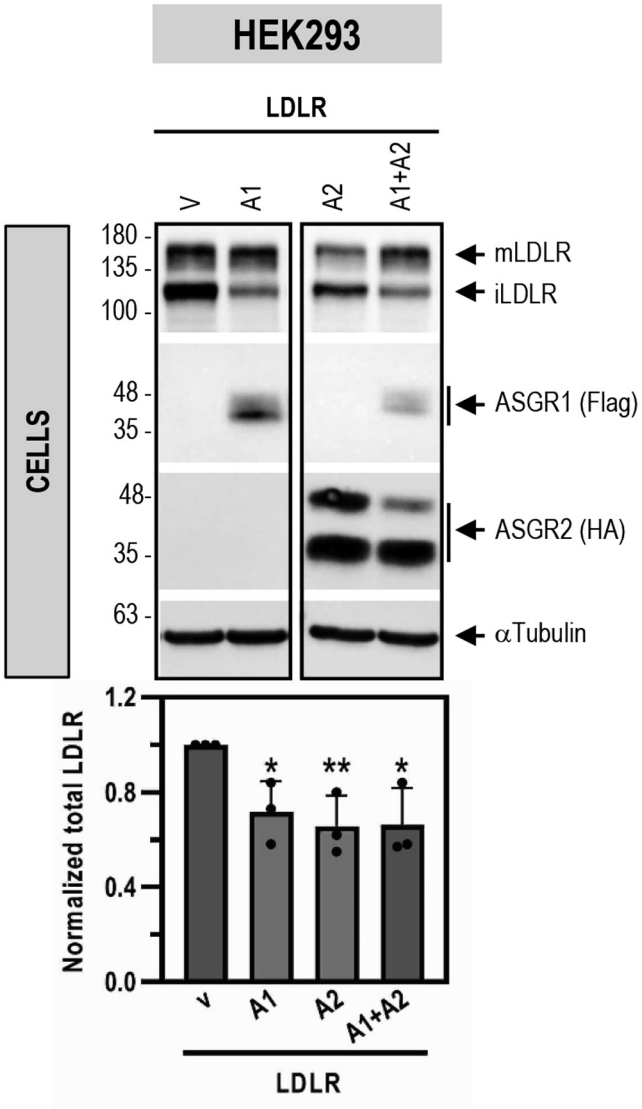

Figure 7. ASGR1 and ASGR2 degrade LDLR under overexpression conditions in HEK293 cells. HEK293 cells were cotransfected with V5-tagged LDLR and Flag-tagged ASGR1 (A1), HA-tagged ASGR2 (A2), or their combination (A1 + A2) or control empty vector (V). Western blot analyses and quantification of cellular LDLR (V5) (V5 antibody), ASGR1 (Flag-HRP), and ASGR2 (HA-HRP) are shown. Data are representative of three independent experiments. Quantifications are averages ±SD. $^{*}p < 0.1$; $^{**}p < 0.01$ (*t* test) are relative to the control vector condition.

Thus, we next probed the interaction of WT ASGR1 or its triple Ala-mutant (QA/WA/EA) with coexpressed LDLR-V5 in HEK293 cells. Immunoprecipitation with Flag antibody (ASGR1-Flag) and WB with antibodies for ASGR1 or LDLR (Fig. 8*C*; left panel) revealed that WT ASGR1 binds to both immature iLDLR (non-O-glycosylated; ∼110 kDa) and mature mLDLR (N- and O-glycosylated; ∼150 kDa) (22). In contrast, the triple Ala-mutant that lost its carbohydrate-binding capacity primarily binds the non-O-glycosylated iLDLR (Fig. 8*C*; left panel). Binding of the LDLR to ASGR1 was further confirmed in a reciprocal binding assay where the LDLR-V5 is immunoprecipitated first with a mAb-V5 and the immune complex is then separated by SDS-PAGE and revealed by WB to ASGR1 (Fig. 8*C*; right panel).

We next investigated whether the enhanced degradation of functional LDLR requires the intact carbohydrate-binding motif of ASGR1. Thus, the levels of cell-surface LDLR and DiI-LDL uptake were estimated in HEK293 cells expressing either LDLR alone or LDLR and ASGR2 together with either WT ASGR1 or its triple Ala-mutant (QA/WA/EA). In nonpermeabilized cells, IF showed that both cell-surface LDLR and DiI-LDL uptake are significantly reduced in the presence of WT ASGR1 but not of its QA/WA/EA triple Ala-mutant (Fig. 9*A*). Thus, functional cell-surface LDLR levels are reduced only by WT ASGR1 and require its critical carbohydrate-binding residues. We extended these data by biotinylating cell-surface proteins of the above HEK293 cells and analyzed the biotinylated proteins by WB. The data showed that the ratio of cell-surface [iLDLR]/[total LDLR] is significantly reduced (∼40%) by WT ASGR1 but not by the triple mutant (Fig. 9*B*; lower left panel). Furthermore, we noticed that the cell-surface levels of the triple-Ala mutant of ASGR1 are ∼60% (∼1.6 fold) higher than the WT (Fig. 9*B*; top left panel), mirroring its ∼70% (∼1.7 fold) increased total cellular levels (Fig. 9*B*; right panel) and suggesting that even at higher levels, this mutant that binds iLDLR (Fig. 8*C*; left panel) does not efficiently reduce LDLR levels (Fig. 9, *A* and *B*). Collectively, the data suggest that the integrity of ASGR1 CRD regulates its ability to reduce the levels of cell-surface iLDLR.

In contrast, WB analyses of the total levels of LDLR in these cells showed that, as for WT, the triple QA/WA/EA and double QA/WA mutants of ASGR1 can also significantly reduce total LDLR levels (∼40%) relative to a vector control lacking ASGR1/2 (Fig. 9*C*; lower right panel). As observed at the plasma membrane (Fig. 9*B*; left panel), in total cell lysate (intracellular and plasma membrane) WT ASGR1 also reduced the levels of iLDLR, which is not seen with the CRD mutants that primarily reduce the levels of mLDLR (Fig. 9*C*; lower left panel). This is evident from the relative ratio of [iLDLR]/[total LDLR], which is ∼40% lower in WT ASGR1 *versus* double or triple mutants and vector control (Fig. 9*C*; lower left panel). Since some of the LDLR is shed into the medium by undefined matrix metalloproteases (23), we also analyzed the fate of media LDLR. The data showed that ASGR1 also reduces the levels of the shed forms of LDLR by carbohydrate-dependent (WT) and carbohydrate-independent (Ala-mutants) activities (Fig. 9*C*; top right panel). Similar analyses in HEK293 cells only overexpressing ASGR1 and/or LDLR-V5 (Fig. S1) mirrored the above results where both ASGR1 and ASGR2 are coexpressed (Fig. 9*C*). This is taken as evidence that, under overexpression conditions, the ASGR1-mediated activity on LDLR *via* its lectin-binding domain is independent of ASGR2. Indeed, silencing ASGR1 in HepG2-PCSK9-KO cells (that still endogenously express ASGR2, Fig. 1*D*) significantly increased total cellular LDLR levels, associated with an ∼3-fold enhanced shedding of the LDLR (∼10% of total LDLR), especially iLDLR (Fig. 9*D*).

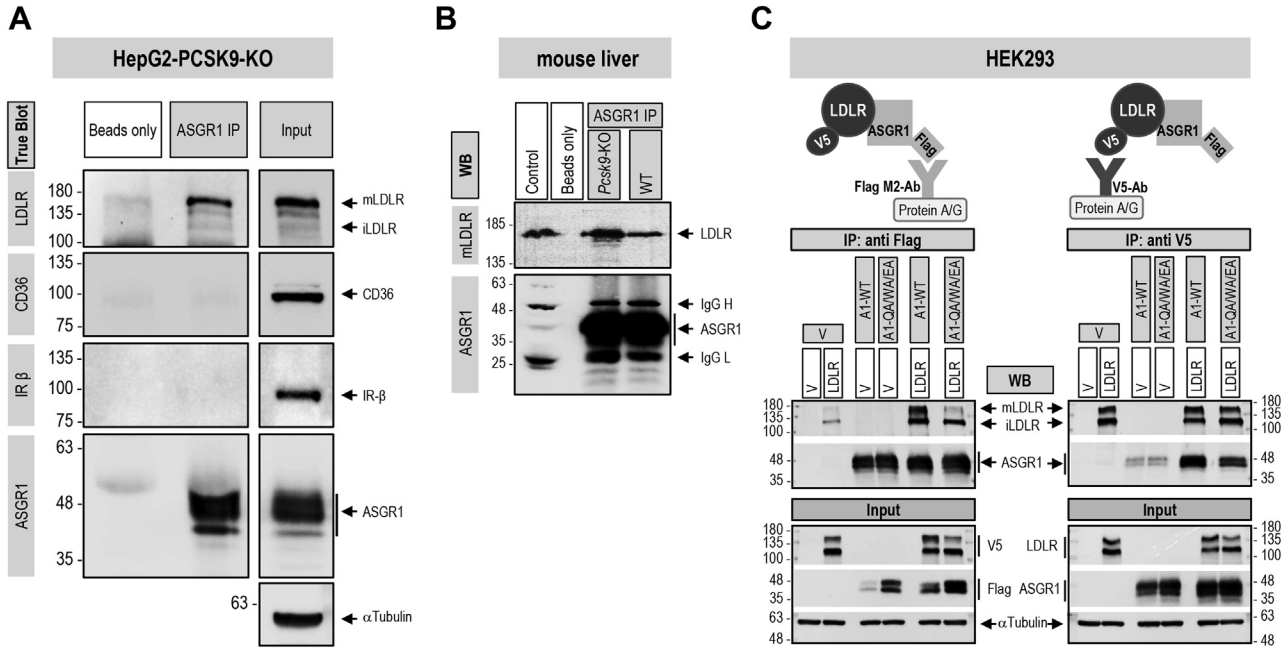

Figure 8. LDLR and ASGR1 form a complex that is not limited to lectin binding. *A*, coimmunoprecipitation of endogenous LDLR and ASGR1 in HepG2-PCSK9-KO cells. Pull-downs with ASGR1 antibody were analyzed by TrueBlot for ASGR1 and LDLR and for CD36 and IR (shown as IR-β) as negative controls for membrane-bound receptors. To "Beads only" negative control addition of ASGR1 antibody was omitted. "Input" represents 10% of the original material subjected to coimmunoprecipitation. *B*, coimmunoprecipitation from liver extracts of WT and *PCSK9*-KO mice. Pull-downs with ASGR1 antibody were analyzed by Western blot for LDLR and ASGR1. To "Beads only" negative control addition of ASGR1 antibody was omitted. "Control" (IgG migration control) consists of WT mouse liver lysate (30 μg) plus ASGR1 antibody. *C*, coimmunoprecipitation from HEK293 cells transfected with vector (V), V5-tagged LDLR or Flag-tagged ASGR1, WT or mutant Q240A/W244A/E253A (QA/WA/EA), or a combination of ASGR1 and LDLR. Pull-downs with Flag M2 antibody (*left panel*) or V5 antibody (*right panel*) were analyzed by Western blot for LDLR and ASGR1. "Input" represents 10% of the original material subjected to coimmunoprecipitation. Data are representative of two independent experiments.

ASGR1 specificity for LDLR

The present data are the first to identify the secretory membrane-bound LDLR as a physiological target of ASGR1, as opposed to soluble desialylated glycoproteins, *e.g.*, von Willebrand factor (24), normally thought to be sensitive to hepatocyte-derived ASGR1 regulation (11). However, since we do not know the repertoire of liver glycoproteins that are targeted by ASGR1, we next investigated the PCSK9-independent ability of ASGR1 to enhance the degradation of other membrane-bound liver receptors. Accordingly, we analyzed by WB the endogenous levels of CD36 and IR-β following KD of ASGR1 in HepG2-PCSK9-KO cells. The data show that, although KD of ASGR1 increased the levels of LDLR by ∼2-fold, those of CD36 and IR-β were not affected (Fig. 10). Thus, even though like the LDLR, the highly N-glycosylated CD36 is a target of PCSK9 (25), it is not sensitive to ASGR1 in the absence of PCSK9. We conclude that the ability of ASGR1 to enhance the degradation of the LDLR may not apply to all liver-derived secretory membrane-bound receptors.

Furin sheds ASGR1

Furin, the third member of the proprotein convertase (PC) family (26), has been shown to enhance the shedding of various cell-surface proteins at the general PC-like motif (**R**/**K**)Xn(**R**/**K**)↓, where Xn represents 0, 2, 4, or 6 spacer aa (27). These include the type II membrane-bound CASC4 and GPP130 implicated in cancer/metastasis (28) and the type I membrane-bound SARS-CoV-2 spike glycoprotein (17). It can also cleave and inactivate PCSK9 in liver hepatocytes (29, 30). Scanning the primary sequence of the luminal domain of human ASGR1 revealed the presence of two potential Furin-like cleavage sites, namely, **R**GL**R**$_{74}$↓ET and **R**KM**K**$_{103}$↓SL. Hence, we addressed the possibility that Furin and/or other PCs could shed ASGR1. Coexpression in HEK293 cells of human ASGR1 with each of the liver-expressed PCs (26) revealed that only Furin can cleave the protein into a soluble ∼28-kDa secreted form (shed ASGR1; Fig. 11*A*). Ala-mutation of the **R**GL**R**$_{74}$↓ET site had no effect (Fig. 11*B*), whereas only Ala-mutation of the underlined basic aa in the **R**KM**K**$_{103}$↓SL site abrogated Furin cleavage and hence shedding of ASGR1 (Fig. 11*C*). Indeed, insertion of an optimal Furin-like site **RRRR**$_{103}$↓**E**L (17, 29) resulted in complete cleavage of mature ∼48-kDa ASGR1 (upper band, likely endoH resistant (17)) by endogenous Furin into a soluble secreted ∼28-kDa sASGR1 (Fig. 11*D*). A comparable processing pattern was observed in hepatic HepG2-PCSK9-KO cells (Fig. 11*E*). In conclusion, Furin sheds ASGR1, possibly resulting in a LOF toward LDLR.

Discussion

The hepatic ASGR is pivotal for the efficient clearance of desialylated glycoproteins from circulation by receptor-mediated endocytosis and lysosomal degradation, whereupon

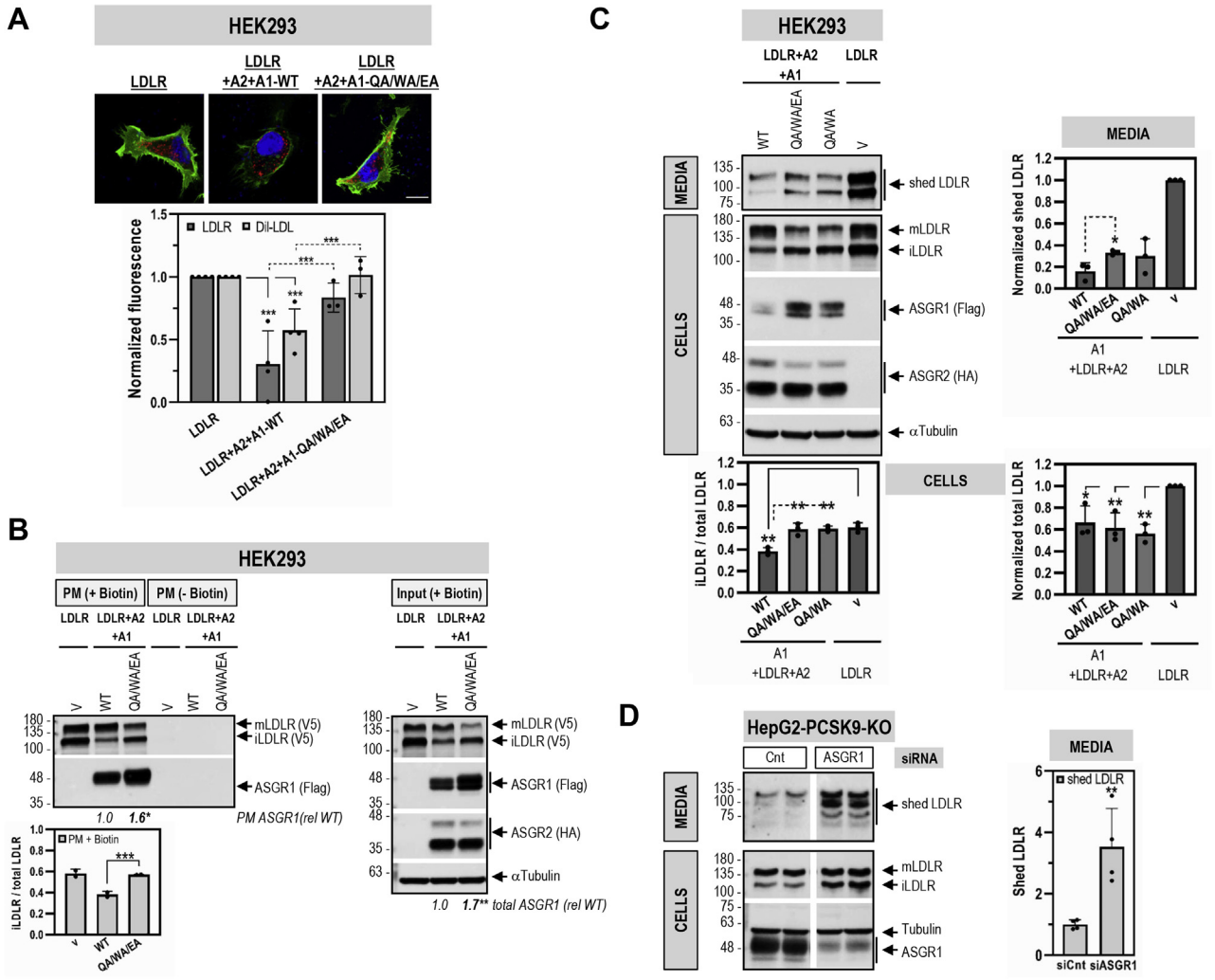

Figure 9. The lectin-binding domain in ASGR1 is important for the ASGR1-mediated degradation of the functional, mainly non-O-glycosylated, LDLR at the plasma membrane. HEK293 cells were transfected with V5-tagged LDLR alone or in combination with HA-tagged ASGR2 and Flag-tagged ASGR1, WT or its carbohydrate-binding mutants Q240A/W244A/E253A (QA/WA/EA) (*A–C*) or Q240A/W244A (QA/WA) (*C*). *A*, immunofluorescence microscopy of plasma membrane–overexpressed LDLR (*green signal*) and Dil-LDL uptake (*red signal*) for 2 h at 37 °C before fixation. Nontransfected cells (V) expressed ∼100-fold less LDLR than transfected ones. The scale bar represents 15 μm. *B*, surface protein biotinylation: cells incubated with Biotin (+Biotin) or PBS (−Biotin) were lysed and plasma membrane (PM) proteins were pulled down with streptavidin and analyzed by Western blot (WB) for LDLR (V5-HRP) and ASGR1 (Flag-HRP) (*left panel*). One-eighth (12.5%; 30 μg) of the (+Biotin) cell lysate before streptavidin pull-down (input) was analyzed by WB (*right panel*). *C*, WB analyses of total cellular LDLR (mature mLDLR and immature iLDLR), ASGR1 (Flag-HRP) and ASGR2 (HA-HRP), and shed LDLR in the media. The WB of the control vector condition (V) is the same as that in Figure 7. This is justified since the above control data are derived from the same experiment testing the effects on LDLR of ASGR2 alone (Fig. 7) and of ASGR1 in the presence (Figs. 7 and 9*C*) or absence of ASGR2 (Fig. 7). *D*, HepG2-PCSK9-KO cells were transfected for 48 h with 20 nM nontargeting (Cnt) siRNA or siRNA ASGR1. WB analyses of total cellular LDLR (mLDLR and iLDLR), ASGR1, and of shed LDLR in the media are shown. Note that 13% of total media and 8% of total lysates are loaded on the gel and that the exposure times are 15 and 3 min, respectively. Data are representative of at least two independent experiments. Quantifications are averages ±SD. *$p < 0.05$; **$p < 0.01$; ***$p < 0.001$ (*t* test).

ASGR is recycled back to the cell surface (13, 31). Glycoprotein ASGR ligands contain terminal galactose or N-acetylgalactosamine, with the latter being the preferred residue (31). In humans, the functional receptor is composed of two subunits, ASGR1 (major, ∼46 kDa) and ASGR2 (minor, ∼50 kDa), that exist as homo-oligomers or hetero-oligomers in a molar ratio of ∼3:1, respectively (13, 31). Both subunits are type II transmembrane proteins comprising a cytosolic, transmembrane domain; a luminal stalk region; and a calcium-dependent CRD (Fig. 1*A*). Oligomerization of the ASGR subunits *via* their respective stalk regions occurs in the ER (31). ASGRs are internalized from the cell surface *via* clathrin-coated vesicles into endosomes and are rapidly recycled constitutively even in the absence of a ligand (11). Thus, at steady state ∼40% to 60% of total cellular ASGRs are on the cell surface (31). So far, the known ligands of ASGRs are soluble desialylated proteins, including von Willebrand factor (11) and exogenous proteins (*e.g.*, asialofuetin, asialoorosomucoid) (32).

Recently, it was observed that conjugation of antisense oligonucleotides to N-acetylgalactosamine mediated their efficient uptake into liver hepatocytes *via* ASGR1, providing a powerful targeted delivery of these and other drugs to the liver (33). Indeed, an ASGR1-targeted antisense siRNA technology is now successfully applied to silence liver PCSK9 in hypercholesterolemic patients worldwide (34).

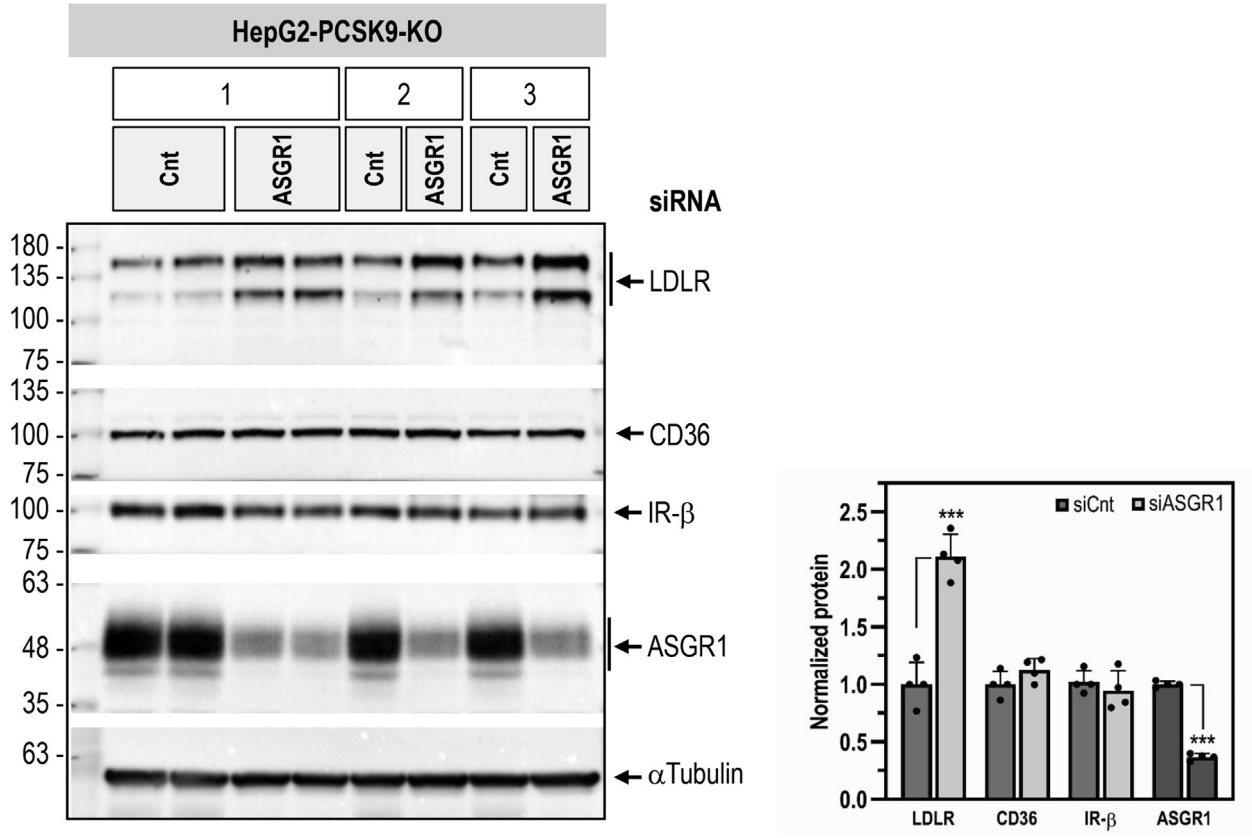

Figure 10. ASGR1 specificity for LDLR. HepG2-PCSK9-KO cells were transfected with 20 nM nontargeting (Cnt) siRNA or siRNA ASGR1 for 48 h. Western blot analyses and quantification of total cellular LDLR, ASGR1, CD36, and IR-β from three independent experiments are shown. Quantifications are averages ±SD. ***$p < 0.001$ (*t* test).

Circulating PCSK9 originating from hepatocytes (2) binds to cell-surface LDLR and targets it to degradation in endosomes/lysosomes (6). This mechanism led to a powerful new treatment to reduce LDLc *via* inhibitory monoclonal antibodies or liver targeted antisense siRNA silencing of its mRNA (35). In 2016, Nioi *et al.* (12) reported that two human *ASGR1*-deletion variants found in Iceland, resulting in truncated proteins, likely inactive, are associated with a modest ∼10% to 14% reduction in LDLc, yet with a significant ∼34% reduced risk of coronary artery disease. This suggested that the atheroprotective effects of *ASGR1* LOF extended beyond reduction of serum LDLc and could implicate extrahepatic functions of ASGR1, *e.g.*, in macrophages (36).

Since PCSK9 is a major player in the regulation of LDLc (7) and its receptor LDLR (3, 6), and ASGR1/LDLR colocalize at the cell surface (Fig. 2*A*), we investigated the possible involvement of ASGR1 in the modulation of the LDLR (11) and/or PCSK9 functions. The data presented in this work clearly eliminated a reciprocal direct effect between PCSK9 and ASGR1 proteins (Figs. 2–5) and demonstrated that loss of endogenous ASGR1 in hepatic cells lines enhanced the levels of the LDLR and its ability to uptake DiI-LDL (Fig. 5), whereas the reverse is true upon overexpression of ASGR1 (Fig. 6), and both phenotypes are independent of PCSK9. This was confirmed *in vivo* in mice lacking PCSK9, which as expected exhibit higher levels of LDLR (18) but no significant change in ASGR1 protein levels (Fig. 3). Finally, lack of endogenous ASGR1 in HepG2 cells does not affect PCSK9 mRNA or its protein levels in cells and media (Fig. 4).

In the absence of PCSK9, co-IP experiments in HepG2-PCSK9-KO cells and in mouse *Pcsk9*-KO livers revealed that endogenous ASGR1 and LDLR form a complex (Fig. 8, *A* and *B*). Since ASGR1 binds galactose/N-acetyl-galactosamine, and its Gln_{240}, Trp_{244}, and Glu_{253} are implicated in carbohydrate recognition (32), we tested the importance of these ASGR1 CRD residues in the regulation of the LDLR. The triple Ala-mutant of these residues largely failed to co-IP with mLDLR (∼150 kDa) in HEK293 cells but still bound non-O-glycosylated iLDLR (∼110 kDa) (Fig. 8*C*; left panel). This unexpected result revealed that ASGR1 could bind mostly the mLDLR (N- and O-glycosylated) in a sugar-dependent fashion and iLDLR (N-glycosylated) in an O-glycosylation-independent manner. These data suggest that the galactose/N-acetyl-galactosamine residues recognized by the CRD of ASGR1 likely reside in part on O-glycosylated chains of the mLDLR. The latter are predominantly present close to the C-terminal transmembrane domain but are also found in the linker regions separating the N-terminal repeat domains of the LDLR (22). Finally, shedding of the LDLR by metalloproteases is thought to mostly target iLDLR (23). Overexpression of WT ASGR1 decreased LDLR shedding, likely due to degradation of mainly iLDLR (Fig. 9*C*), and silencing endogenous ASGR1

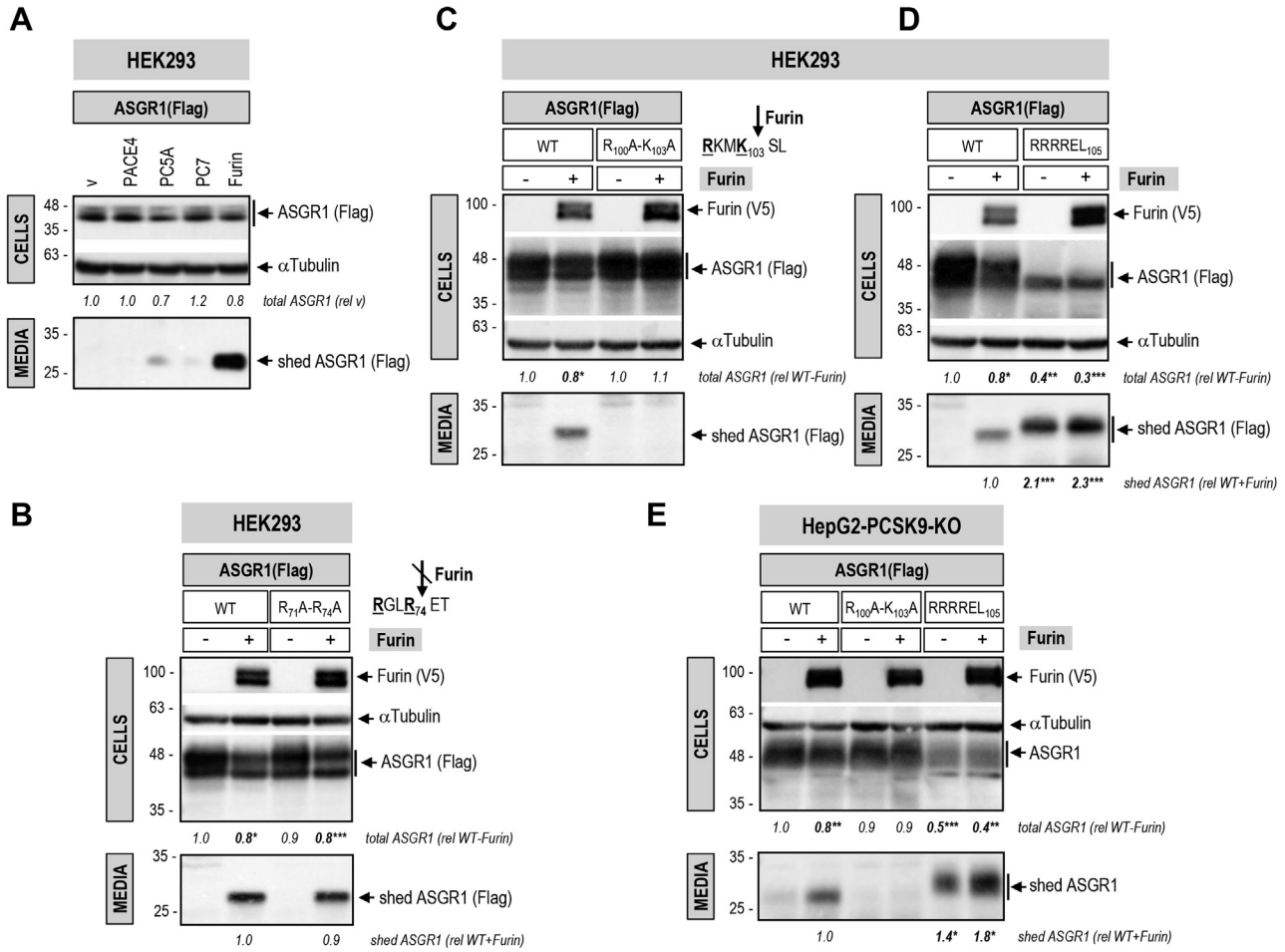

Figure 11. ASGR1 is shed in the media by Furin. *A*, HEK293 cells were cotransfected with Flag-tagged ASGR1 and one of the liver-expressed PCs, PACE4, PC5A, PC7, Furin, or empty vector (V), as negative control. Western blot analyses of cellular ASGR1 (Flag-HRP) and of shed ASGR1 (Flag-HRP) in the media are shown. HEK293 cells (*B–D*) or HepG2-PCSK9-KO cells (*E*) were cotransfected with Flag-tagged ASGR1, WT or Furin-like cleavage site mutants $R_{71}A\text{-}R_{74}A$ (*B*), $R_{100}A\text{-}K_{103}A$ (*C* and *E*), $RRRREL_{105}$ (*D* and *E*), and V5-tagged Furin (+) or empty vector (–). Western blot analyses of cellular Furin (V5-HRP) and ASGR1 (Flag-HRP) and of shed ASGR1 (Flag-HRP) in the media are depicted (*B–D*). For HepG2-PCSK9-KO cells, ASGR1 in cells and media is revealed with ASGR1 antibody (*E*). The slower SDS-PAGE migration of shed ASGR1 $RRRREL_{105}$ mutant in (*D*) and (*E*) is likely due to an increased negative charge (glutamic acid, E) following the Furin cleavage site in mutant protein $RRRR_{103}\downarrow$ELE compared with WT $RKMK_{103}\downarrow$SLE. Data are representative of three independent experiments. Quantifications are averages ±SD. $^*p < 0.05$; $^{**}p < 0.01$; $^{***}p < 0.001$ (*t* test).

resulted in elevated shedding of primarily iLDLR, in line with increased cellular LDLR and higher exposure to endogenous sheddase(s) (Fig. 9*D*). Thus, both ASGR1-induced degradation of the LDLR and the cell-surface shedding of the latter mostly target iLDLR, whereas PCSK9 targets both LDLR forms. It was of interest to note that not all cell-surface glycoproteins are targeted by ASGR1, since the endogenous IR and CD36 in HepG2 cells were insensitive to it (Fig. 10), possibly because of their low levels of desialylation.

The nine-membered family of PCs is composed of secretory serine proteases implicated in a wide variety of functions both in health and disease (26, 37). The first seven members of the family cleave substrates at the canonical motif **R/K**-Xn-**R/K**↓, where Xn = 0, 2, 4, or 6 spacer aa (26). The presence of two such motifs in the primary sequence of ASGR1 suggested that it may be cleaved by one or more member(s) of the PC family. Our data showed that only Furin can cleave ASGR1 at $\underline{\mathbf{R}}KM\underline{\mathbf{K}}_{103}\downarrow SL$ and shed it into the media (Fig. 11, *A*, *C* and *E*) but it does not process the other $\underline{\mathbf{R}}GL\underline{\mathbf{R}}_{74}$ - ET site (Fig. 11*B*). We therefore expect that some of the hepatic ASGR1 may be circulating in plasma as a soluble shed ASGR1 form (aa 104–291) that still encodes the CRD with its critical residues (Gln_{240}, Trp_{244}, and Glu_{253}) and conceivably could bind to nonhepatic targets and regulate their function. The generation of an optimally shed form of ASGR1 with the above sequence replaced by $\underline{\mathbf{RRRR}}_{103}\downarrow\underline{\mathbf{E}}L$ (Fig. 11, *D* and *E*) may lead in the future to the identification of some of the possible extrahepatic roles of the resulting circulating ASGR1. For example, the lack of ASGR1 in human was suggested to possibly affect receptors implicated in modulating inflammation (12).

Finally, it is interesting to note that liver ASGR1 has recently been shown to bind the N-terminal domain and ACE2 receptor binding domain of the Spike-glycoprotein of SARS-CoV-2 (38), the etiological agent of COVID-19 (39). Since liver does not significantly express ACE2, the main SARS-CoV-2 receptor (40), it is possible that ASGR1 can act as an alternative receptor in hepatocytes, thereby expanding the tropism of this deadly virus (41). It would thus be informative

to define the mode of interaction of ASGR1 with the Spike-glycoprotein of SARS-CoV-2 and whether the LDLR may participate in this process.

We conclude that the LDLR is a ligand of hepatic ASGR1, representing the first case of a membrane-bound protein targeted by ASGR1 for degradation, since ASGRs are primarily known to interact with circulating factors (11, 31). Our data provide a mechanism for the modest reduction of LDLc in humans lacking functional ASGR1 (12). The other functions of ASGR1 that are not related to LDLc regulation but affect inflammation, atherosclerosis, and cardiovascular health (12) are yet to be identified.

Experimental procedures

Plasmids and site-directed mutagenesis

The cDNAs encoding for human ASGR1 and human ASGR2 were obtained from GenScript. Human ASGR1 and its mutants (Q240A/W244A and Q240A/W244A/E253A) and human ASGR2 were subcloned into pcDNA 3.1 vector (Invitrogen) containing a C-terminal Flag tag (ASGR1) or HA tag (ASGR2). Point mutations of ASGR1 were created by site-directed mutagenesis, and the identity of each mutant was confirmed by DNA sequencing. The constructions containing the human LDLR, human PACE4, human PC7, human Furin, or mouse PC5A, cloned in pIRES2-EGFP (Clontech), were described (42, 43).

Cell culture, transfections, and treatments

HepG2 (human hepatocellular carcinoma), HepG2-PCSK9-KO (CRISPR-Cas9 for PCSK9), IHH (immortalized human primary hepatocytes), and HEK293 (human embryonic kidney-derived epithelial) cells were cultured at 37 °C under 5% CO_2 in complete medium (Eagle's Minimal Essential Medium for HepG2 and IHH cells; Dulbecco's Modified Eagle's Medium for HEK293 cells) (Gibco, ThermoFisher Scientific) containing 10% (v/v) fetal bovine serum (Invitrogen).

Protein overexpression was achieved using JetPEI (PolyPlus) transfection reagent in HepG2 and HepG2-PCSK9-KO cells (2 μg total DNA/well in 12-well plate) and JetPRIME (PolyPlus) in HEK293 cells (1 μg total DNA/well in 12-well plate), following the manufacturer's recommendations. Twenty-four hours post transfection, the culturing medium was changed from complete to serum-free to achieve maximal expression of the LDLR, and the cells were treated according to each experiment. Incubations with *exogenous* purified PCSK9 (ACRO Biosytems) were carried out for an additional 20 h. LDLR functionality was assessed by incubation with DiI-LDL (Alfa Aesar, Kalen Biochemicals). Small interfering RNAs (siRNAs) targeted against ASGR1 or PCSK9 were purchased from siGenome, Horizon Discoveries, and transfections were carried out using INTERFERin (PolyPlus) as per manufacturer's instructions.

Western blotting

Cells were washed twice with ice-cold PBS and lysed 60 min on ice with ice-cold nondenaturing cell lysis buffer (20 mM Tris-HCl, pH 8, 137 mM NaCl, 2 mM Na_2EDTA, 1% Nonidet P-40, 10% glycerol, supplemented with protease inhibitor cocktail without EDTA). Mouse livers were homogenized, and protein extraction was performed in radioimmune precipitation assay buffer (50 mM Tris-HCl pH 7.8, 150 mM NaCl, 1% Nonidet P-40, 0.5% sodium deoxycholate, 0.1% SDS, supplemented with complete protease inhibitor cocktail) for 40 min on ice. Cell lysates (20–30 μg of total protein) and conditioned media (20% of total media) were electrophoretically resolved on 8% or 10% Tris-glycine SDS-polyacrylamide gels, respectively, and transferred to PVDF membranes using a Trans-Blot Turbo Transfer System (Bio-Rad). Mouse liver lysates were subjected to 8% Tris-tricine SDS-PAGE before transfer to PVDF membrane. Membranes were blocked with 5% skim milk in Tris-buffered saline containing Tween-20 for 1 h and subsequently incubated with primary antibody according to the manufacturer's recommendations. Antigen–primary antibodies complexes were detected with secondary antibodies conjugated to horse radish peroxidase and developed using a chemiluminescent reagent (Clarity ECL, Bio-Rad). Images of the WBs were acquired using a ChemiDoc MP System (Bio-Rad) and analyzed with Image Lab (version 6.0) software (Bio-Rad). Immunoblots from cell lysates and liver lysates were quantified and normalized to membranes probed for α-Tubulin or β-Actin, respectively. See Table S1 for a list of the antibodies used for WB analyses. In all figures, immunoblots were cropped for clarity.

Immunofluorescence

For immunofluorescence experiments, HEK293, HepG2, or HepG2-PCSK9-KO cells (0.5×10^5 cells/well) were plated on poly-L-lysine–coated round microscope coverslips that were placed in a 24-well cell culture plate. Cells were then treated as required for each experiment (PCSK9 incubation, siRNA transfection, protein overexpression). To analyze plasma membrane LDLR expression, the cells were washed twice with PBS and fixed with a solution of 4% paraformaldehyde in PBS (10 min). After blocking with PBS + 2% bovine serum albumin (BSA) (1 h), samples were incubated at 4 °C overnight with the respective primary antibodies (see Table S1), washed with PBS, and incubated with the appropriate fluorescent secondary antibody (see Table S1) for 1 h at room temperature. To analyze cell-surface ASGR1, cells were incubated in SFM media with ASGR1 antibody (1/50) for 2 h at 37 °C. Cells were then fixed and incubated with appropriate secondary antibodies as described above. When LDLR functionality was tested, prior to fixation cells were incubated for 2 h at 37 °C with 5 μg/ml DiI-LDL in SFM media. Coverslips were mounted on a glass slide with ProLong Gold antifade reagent with DAPI. Samples were visualized using a Plan-Apochromat 63x 1.4 oil objective of an LSM-710 confocal laser scanning microscope (Carl Zeiss) with sequential excitation and capture image acquisition with a digital camera. Images were processed with ZEN software. Image analysis to quantify the fluorescence intensities was accomplished using Volocity 6.0.

Animal experiments

In situ hybridization studies of ASGR1 and ASGR2 mRNA expression were performed on whole-body tissue cryostat sections (8–10 μm) from WT (C57BL/6J) mice, embryonic day 10 to adult, as described (2, 15, 44). Mouse antisense and sense (negative control) cRNA (complementary RNA) riboprobes coding for ASGR1 and ASGR2 were labeled with ^{35}S-UTP and ^{35}S-CTP (1250 Ci/mmol; Amersham Pharmacia), to obtain high specific activities of ≈1000 Ci/mmol (2). All studies on mouse tissues were approved by the IRCM ethics committee.

Immunohistochemistry in mouse liver sections

LDLR and ASGR1 protein expression in mouse liver was assessed by IHC on cryosections (9–10 mice) and WB of tissue extracts (3–4 mice) from 12- to 16-week-old male *Pcsk9*$^{-/-}$ and *Ldlr*$^{-/-}$ mice on a C57BL/6J background and age-matched C57BL/6J controls. For IHC, mice liver cryosections (8 μm thick) were fixed in 4% paraformaldehyde in PBS for 1 h, rinsed in PBS with 0.1% glycine, washed in PBS, and blocked in 1% BSA (Sigma-Aldrich) in PBS for 1 h at room temperature. Sections were then incubated overnight at 4 °C with the LDLR and ASGR1 primary antibodies (see Table S1) and washed three times for a total of 15 min in PBS. Labeling was visualized by incubation with Alexa Fluor 488–labeled secondary antibodies (see Table S1) for 1 h at room temperature in PBS. After three washes with PBS, nuclei were counterstained with Hoechst dye (Sigma-Aldrich). Images were acquired as described previously using an LSM 700 confocal microscope equipped with ZEN 2011 software (45). Data quantification was achieved using Matlab software. For all images the minimum threshold was set to a value of 20, negative control values were subtracted, and final values were analyzed using Microsoft Excel. For each genotype, the most representative image was chosen.

Quantitative RT-PCR

Quantitative RT-PCR was performed as described (18). Briefly, total RNA from liver or cells was extracted with TRIzol (Invitrogen). cDNA was generated from 1 μg of total RNA using a SuperScript IV cDNA reverse transcriptase (Invitrogen). Quantitative PCR was performed using the SYBR Select Master Mix (Applied Biosystems) and the ΔΔct method. Expression of each human gene was normalized to that of Tata-binding protein (TBP), whereas expression of the mouse genes was normalized to that of hypoxanthine phosphoribosyl transferase (HPRT). The sets of primers (ThermoFisher Scientific) were as follows: human ASGR1, 5′-GGGAAGAAAGATGAAGTCGCTAGA *versus* 5′-GCAGGCTGGAGTGATCTTCAC; human ASGR2, 5′- GACGGAGGTCCAGGCAATC *versus* 5′- TGGCTCCTAGGGATGTGATCTT; human LDLR, 5′- AGGAGACGTGCTTGTCTGTC *versus* 5′-CTGAGCCGTTGTCGCAGT; human PCSK9, 5′- TGGAGCTGGCCTTGAAGTTG *versus* 5′- GATGCTCTGGGCAAAGACAGA; human SREPB2, 5′- AGAATGTCCTTCTGATGTCC *versus* 5′- GGAGAGTCTGGCTCATCTT; human TBP, 5′- CGAATATAATCCCAAGCGGTTT *versus* 5′- GTGGTTCGTGGCTCTCTTATCC; mouse ASGR1, 5′- TCTGACGTGCGAAGCTTGAG *versus* 5′-GGTCCTTTCAGAGCCATTGC; mouse ASGR, 5′- CGATGATGAACATGGCTCTCA *versus* 5′-AGGCTGCCCTTTCCAGTGT; mouse HPRT, 5′- CCGAGGATTTGGAAAAAGTGTT *versus* 5′-CCTTCATGACATCTCGAGCAAGT.

Coimmunoprecipitation

For co-IP of LDLR–ASGR1 complexes from HepG2-PCSK9-KO cells (endogenous LDLR–ASGR1 complex) and transfected HEK293 cells, cells were lysed in Pierce nondenaturing IP buffer supplemented with complete protease inhibitor cocktail. Lysates containing 0.5 mg total protein (HepG2-PCSK9-KO cells) or 0.25 mg total protein (HEK293 cells) were exposed overnight, at 4 °C on a rocker, to 2 μg of IP antibody (rabbit anti-ASGR1 antibody for HepG2-PCSK9-KO cell lysates; mouse (IgG1)MAB Flag M2 or mouse (IgG2a) anti-V5 MAB antibodies for HEK293 cell lysates). On the following day, 60 μl True Blot anti-rabbit IgG beads (HepG2-PCSK9-KO cell lysates) or 40 μl of protein A/G PLUS-Agarose (HEK293 cell lysates) were added for an additional 1 to 2 h incubation. Following three washes with lysis buffer/protease inhibitors and two washes with PBS and elution in 70 μl 2× Laemmli sample buffer, the pull-downs were separated by 8% Tris-glycine SDS-PAGE along with inputs (10% of original material used for co-IP) and analyzed by WB for LDLR and ASGR1 using their respective primary antibodies. In the case of LDLR–ASGR1 co-IP from HepG2-PCSK9-KO cell lysates, separate pull-downs were also analyzed for endogenous CD36 and IR as negative controls for membrane-bound receptors. Rabbit IgG TrueBlot was used for the detection of immunoblotted ASGR1 from HepG2-PCSK9-KO cell lysates (endogenous LDLR-ASGR1 complex), which eliminated the hindrance by interfering immunoprecipitating immunoglobulin heavy and light chains. TrueBlot preferentially detects the nonreduced form of rabbit IgG over the reduced, SDS-denatured form of IgG.

For co-IP of LDLR-ASGR1 complexes from mice livers, fresh livers from *Pcsk9*-KO mice littermates were lysed in Pierce nondenaturing IP buffer supplemented with complete protease inhibitor mixture. Liver lysates containing 1 mg of total protein were exposed to 2 μg of rabbit anti-ASGR1 antibody overnight at 4 °C on a rocker. The following morning, 100 μl of Surebeads Protein G magnetic beads (Bio-Rad) was added to each sample tube, including “beads only” negative control. Isolation and purification was carried out using magnets as per manufacturer’s instructions. A “control” was included, which consisted of a liver lysate from a wildtype (C57BL/6J) mouse to which ASGR1 antibody was added to help identify the IgGs. See Table S1 for antibodies used.

Cell-surface biotinylation

Biochemical detection of cell-surface LDLR and ASGR1 by WB analysis was performed following the protocol described in (46). Namely, HEK293 cells seeded in six-well plates and after reaching 80% confluency were transiently cotransfected

with 1.5 μg DNA consisting of V5-tagged LDLR and empty vector or a combination of LDLR-V5, HA-tagged ASGR2 and Flag-tagged ASGR1, WT or carbohydrate-binding mutants Q240A/W244A/E253A or Q240A/W244A. Following 48 h post transfection, cells were washed twice with ice-cold PBS and biotinylated with 2 ml of EZ-link sulfo-NHS-LC-Biotin (ThermoScientific 0021335) (0.5 mg/ml in PBS) for 20 min at 4 °C, on ice. After 10 min incubation on ice with ice-cold BSA (0.1 mg/ml) in PBS to quench the reaction and two washes with cold PBS, cells were lysed for 10 min on ice in biotinylation lysis buffer (20 mM Tris pH 7.5, 5 mM EDTA, 5 mM EGTA, 0.5% N-dodecyl-N-maltoside, supplemented with protease inhibitor cocktail without EDTA). Cell lysates were collected after centrifugation at 3000 rpm for 10 min at 4 °C and quantified for protein concentration. Biotinylated cell-surface proteins (240 μg total protein) were immunoprecipitated overnight with 30 μl Streptavidin agarose. Following centrifugation at 7000 rpm for 2 min at 4 °C, the pellet containing the plasma membrane pool was washed three times, eluted in 60 μl 2× Laemmli sample buffer and separated by 8% Tris-glycine SDS-PAGE. A negative control (-Biotin) was included, to which PBS was added instead of Biotin at the biotinylation step. Total proteins (plasma membrane + intracellular) were detected from a fraction of the lysates before Streptavidin immunoprecipitation, which was referred to as "input."

Statistical analysis and graphical representation

Quantifications are defined as averages ±SD. The statistical significance was evaluated by Student's *t* test, and probability values (p) <0.05 were considered significant. Data representation was performed using GraphPad Prism 8 software.

Data availability

All data are contained within the article.

Supporting information—This article contains supporting information (23).

Acknowledgments—Financial support from the Research Institute of St. Joe's Hamilton is acknowledged. We are grateful to B. Mary and H. Oueslati for efficacious editorial assistance.

Author contributions—D. S.-R., R. C. A., N. G. S., and E. G. conceptualization; D. S.-R., E. G., R. E., A. R., J. M., R. M. D., A. E., P. F. L., and N. G. S. methodology; D. S.-R. and N. G. S. software; D. S.-R., E. G., R. E., A. R., R. M. D., P. F. L., and N. G. S. validation; D. S.-R., E. G., R. C. A., and N. G. S. formal analysis; D. S.-R., E. G., R. E., J. M., A. E., J. H. B., P. F. L., R. C. A., N. G. S., R. M. D., and A. R. investigation; R. E., J. M., R. M. D., P. F. L., R. C. A., and N. G. S. resources; D. S.-R., E. G., A. R., J. M., and N. G. S. data curation; D. S.-R., E. G., P. F. L., R. C. A., and N. G. S. writing – original draft; D. S.-R., E. G., P. F. L., R. C. A., and N. G. S. writing – review & editing; D. S.-R., E. G., J. M., and N. G. S. visualization; R. C. A. and N. G. S. supervision; R. C. A. and N. G. S. project administration; R. C. A. and N. G. S. funding acquisition.

Funding and additional information—This work was supported in part by research grants to N. G. S. from the CIHR Foundation Scheme grant (148363), a Canada Research Chair (950-231335), and a Leducq Foundation grant (13 CVD 03), as well as to R. C. A. from the Heart and Stroke Foundation of Canada (G-13-0003064, G-15-0009389) and the Canadian Institutes of Health Research (74477, 173520).

Conflict of interest—The authors declare that they have no conflicts of interest with the contents of this article. R. C. A. is a Career Investigator of the Heart and Stroke Foundation of Ontario and holds the Amgen Canada Research Chair in the Division of Nephrology at St. Joseph's Healthcare and McMaster University.

Abbreviations—The abbreviations used are: ASGR, asialoglycoprotein receptor; CRD, carbohydrate recognition domain; CVD, cardiovascular disease; ER, endoplasmic reticulum; IF, immunofluorescence; IHC, immunohistochemistry; IR, insulin receptor; LDLc, low-density lipoprotein cholesterol; LDLR, low-density lipoprotein receptor; LOF, loss of function; PC, proprotein convertase; PCSK9, proprotein convertase subtilisin/kexin type 9.

References

1. Wadhera, R. K., Steen, D. L., Khan, I., Giugliano, R. P., and Foody, J. M. (2016) A review of low-density lipoprotein cholesterol, treatment strategies, and its impact on cardiovascular disease morbidity and mortality. *J. Clin. Lipidol.* **10**, 472–489
2. Seidah, N. G., Benjannet, S., Wickham, L., Marcinkiewicz, J., Jasmin, S. B., Stifani, S., Basak, A., Prat, A., and Chretien, M. (2003) The secretory proprotein convertase neural apoptosis-regulated convertase 1 (NARC-1): Liver regeneration and neuronal differentiation. *Proc. Natl. Acad. Sci. U. S. A.* **100**, 928–933
3. Maxwell, K. N., and Breslow, J. L. (2004) Adenoviral-mediated expression of Pcsk9 in mice results in a low-density lipoprotein receptor knockout phenotype. *Proc. Natl. Acad. Sci. U. S. A.* **101**, 7100–7105
4. Cohen, J., Pertsemlidis, A., Kotowski, I. K., Graham, R., Garcia, C. K., and Hobbs, H. H. (2005) Low LDL cholesterol in individuals of African descent resulting from frequent nonsense mutations in PCSK9. *Nat. Genet.* **37**, 161
5. McNutt, M. C., Lagace, T. A., and Horton, J. D. (2007) Catalytic activity is not required for secreted PCSK9 to reduce low density lipoprotein receptors in HepG2 cells. *J. Biol. Chem.* **282**, 20799–20803
6. Seidah, N. G., Abifadel, M., Prost, S., Boileau, C., and Prat, A. (2017) The proprotein convertases in hypercholesterolemia and cardiovascular diseases: Emphasis on proprotein convertase subtilisin/kexin 9. *Pharmacol. Rev.* **69**, 33–52
7. Abifadel, M., Varret, M., Rabes, J. P., Allard, D., Ouguerram, K., Devillers, M., Cruaud, C., Benjannet, S., Wickham, L., Erlich, D., Derre, A., Villeger, L., Farnier, M., Beucler, I., Bruckert, E., *et al.* (2003) Mutations in PCSK9 cause autosomal dominant hypercholesterolemia. *Nat. Genet.* **34**, 154–156
8. Cohen, J. C., Boerwinkle, E., Mosley, T. H., Jr., and Hobbs, H. H. (2006) Sequence variations in PCSK9, low LDL, and protection against coronary heart disease. *N. Engl. J. Med.* **354**, 1264–1272
9. Sabatine, M. S., Leiter, L. A., Wiviott, S. D., Giugliano, R. P., Deedwania, P., De Ferrari, G. M., Murphy, S. A., Kuder, J. F., Gouni-Berthold, I., Lewis, B. S., Handelsman, Y., Pineda, A. L., Honarpour, N., Keech, A. C., Sever, P. S., *et al.* (2017) Cardiovascular safety and efficacy of the PCSK9 inhibitor evolocumab in patients with and without diabetes and the effect of evolocumab on glycaemia and risk of new-onset diabetes: A prespecified analysis of the FOURIER randomised controlled trial. *Lancet Diabetes Endocrinol.* **5**, 941–950
10. Ashwell, G., and Harford, J. (1982) Carbohydrate-specific receptors of the liver. *Annu. Rev. Biochem.* **51**, 531–554

11. Igdoura, S. A. (2017) Asialoglycoprotein receptors as important mediators of plasma lipids and atherosclerosis. *Curr. Opin. Lipidol.* **28**, 209–212
12. Nioi, P., Sigurdsson, A., Thorleifsson, G., Helgason, H., Agustsdottir, A. B., Norddahl, G. L., Helgadottir, A., Magnusdottir, A., Jonasdottir, A., Gretarsdottir, S., Jonsdottir, I., Steinthorsdottir, V., Rafnar, T., Swinkels, D. W., Galesloot, T. E., *et al.* (2016) Variant ASGR1 associated with a reduced risk of coronary artery disease. *N. Engl. J. Med.* **374**, 2131–2141
13. Bischoff, J., and Lodish, H. F. (1987) Two asialoglycoprotein receptor polypeptides in human hepatoma cells. *J. Biol. Chem.* **262**, 11825–11832
14. Tabula Muris Consortium, Overall Coordination, Logistical Coordination, Organ Collection and Processing, Library Preparation and Sequencing, Computational Data Analysis, Cell Type Annotation, Writing Group, Supplemental Text Writing Group, and Principal Investigators. (2018) Single-cell transcriptomics of 20 mouse organs creates a Tabula Muris. *Nature* **562**, 367–372
15. Ben Djoudi Ouadda, A., Gauthier, M. S., Susan-Resiga, D., Girard, E., Essalmani, R., Black, M., Marcinkiewicz, J., Forget, D., Hamelin, J., Evagelidis, A., Ly, K., Day, R., Galarneau, L., Corbin, F., Coulombe, B., *et al.* (2019) Ser-phosphorylation of PCSK9 (proprotein convertase subtilisin-kexin 9) by Fam20C (family with sequence similarity 20, member C) kinase enhances its ability to degrade the LDLR (low-density lipoprotein receptor). *Arterioscler. Thromb. Vasc. Biol.* **39**, 1996–2013
16. Susan-Resiga, D., Girard, E., Kiss, R. S., Essalmani, R., Hamelin, J., Asselin, M. C., Awan, Z., Butkinaree, C., Fleury, A., Soldera, A., Dory, Y. L., Baass, A., and Seidah, N. G. (2017) The proprotein convertase subtilisin/kexin type 9-resistant R410S low density lipoprotein receptor mutation: A novel mechanism causing familial hypercholesterolemia. *J. Biol. Chem.* **292**, 1573–1590
17. [preprint] Essalmani, R., Jain, J., Susan-Resiga, D., Andréo, U., Evagelidis, A., Derbali, R. M., Huynh, D. N., Dallaire, F., Laporte, M., Delpal, A., Sutto-Ortiz, P., Coutard, B., Mapa, C., Wilcoxen, K., Decroly, E., *et al.* (2021) Implications of spike-glycoprotein processing at S1/S2 by furin, at S2' by furin and/or TMPRSS2 and shedding of ACE2: Cell-to-cell fusion, cell entry and infectivity of SARS-CoV-2. *bioRxiv*. https://doi.org/10.1101/2020.12.18.423106
18. Zaid, A., Roubtsova, A., Essalmani, R., Marcinkiewicz, J., Chamberland, A., Hamelin, J., Tremblay, M., Jacques, H., Jin, W., Davignon, J., Seidah, N. G., and Prat, A. (2008) Proprotein convertase subtilisin/kexin type 9 (PCSK9): Hepatocyte-specific low-density lipoprotein receptor degradation and critical role in mouse liver regeneration. *Hepatology* **48**, 646–654
19. Gupta, N., Fisker, N., Asselin, M. C., Lindholm, M., Rosenbohm, C., Orum, H., Elmen, J., Seidah, N. G., and Straarup, E. M. (2010) A locked nucleic acid antisense oligonucleotide (LNA) silences PCSK9 and enhances LDLR expression *in vitro* and *in vivo*. *PLoS One* **5**, e10682
20. Dubuc, G., Chamberland, A., Wassef, H., Davignon, J., Seidah, N. G., Bernier, L., and Prat, A. (2004) Statins upregulate PCSK9, the gene encoding the proprotein convertase neural apoptosis-regulated convertase-1 implicated in familial hypercholesterolemia. *Arterioscler. Thromb. Vasc. Biol.* **24**, 1454–1459
21. Roubtsova, A., Chamberland, A., Marcinkiewicz, J., Essalmani, R., Fazel, A., Bergeron, J. J., Seidah, N. G., and Prat, A. (2015) PCSK9 deficiency unmasks a sex/tissue-specific subcellular distribution of the LDL and VLDL receptors in mice. *J. Lipid Res.* **56**, 2133–2142
22. Pedersen, N. B., Wang, S., Narimatsu, Y., Yang, Z., Halim, A., Schjoldager, K. T., Madsen, T. D., Seidah, N. G., Bennett, E. P., Levery, S. B., and Clausen, H. (2014) Low density lipoprotein receptor class A repeats are O-glycosylated in linker regions. *J. Biol. Chem.* **289**, 17312–17324
23. Nassoury, N., Blasiole, D. A., Tebon, O. A., Benjannet, S., Hamelin, J., Poupon, V., McPherson, P. S., Attie, A. D., Prat, A., and Seidah, N. G. (2007) The cellular trafficking of the secretory proprotein convertase PCSK9 and its dependence on the LDLR. *Traffic* **8**, 718–732
24. Ward, S. E., O'Sullivan, J. M., Drakeford, C., Aguila, S., Jondle, C. N., Sharma, J., Fallon, P. G., Brophy, T. M., Preston, R. J. S., Smyth, P., Sheils, O., Chion, A., and O'Donnell, J. S. (2018) A novel role for the macrophage galactose-type lectin receptor in mediating von Willebrand factor clearance. *Blood* **131**, 911–916
25. Demers, A., Samani, S., Lauzier, B., Des Rosiers, C., Sock, E. T., Ong, H., and Mayer, G. (2015) PCSK9 induces CD36 degradation and affects long-chain fatty acid uptake and triglyceride metabolism in adipocytes and in mouse liver. *Arterioscler. Thromb. Vasc. Biol.* **35**, 2517–2525
26. Seidah, N. G., and Prat, A. (2012) The biology and therapeutic targeting of the proprotein convertases. *Nat. Rev. Drug Discov.* **11**, 367–383
27. Lichtenthaler, S. F., Lemberg, M. K., and Fluhrer, R. (2018) Proteolytic ectodomain shedding of membrane proteins in mammals-hardware, concepts, and recent developments. *EMBO J.* **37**, e99456
28. Duval, S., Abu-Thuraia, A., Elkholi, I. E., Chen, R., Seebun, D., Mayne, J., Côté, J. F., Figeys, D., and Seidah, N. G. (2020) Shedding of cancer susceptibility candidate 4 by the convertases PC7/furin unravels a novel secretory protein implicated in cancer progression. *Cell Death Dis.* **11**, 665
29. Benjannet, S., Rhainds, D., Hamelin, J., Nassoury, N., and Seidah, N. G. (2006) The proprotein convertase PCSK9 is inactivated by furin and/or PC5/6A: Functional consequences of natural mutations and post-translational modifications. *J. Biol. Chem.* **281**, 30561–30572
30. Essalmani, R., Susan-Resiga, D., Chamberland, A., Abifadel, M., Creemers, J. W., Boileau, C., Seidah, N. G., and Prat, A. (2011) *In vivo* evidence that furin from hepatocytes inactivates PCSK9. *J. Biol. Chem.* **286**, 4257–4263
31. Weigel, P. H., and Yik, J. H. (2002) Glycans as endocytosis signals: The cases of the asialoglycoprotein and hyaluronan/chondroitin sulfate receptors. *Biochim. Biophys. Acta* **1572**, 341–363
32. Meier, M., Bider, M. D., Malashkevich, V. N., Spiess, M., and Burkhard, P. (2000) Crystal structure of the carbohydrate recognition domain of the H1 subunit of the asialoglycoprotein receptor. *J. Mol. Biol.* **300**, 857–865
33. Tanowitz, M., Hettrick, L., Revenko, A., Kinberger, G. A., Prakash, T. P., and Seth, P. P. (2017) Asialoglycoprotein receptor 1 mediates productive uptake of N-acetylgalactosamine-conjugated and unconjugated phosphorothioate antisense oligonucleotides into liver hepatocytes. *Nucleic Acids Res.* **45**, 12388–12400
34. Stoekenbroek, R. M., Kallend, D., Wijngaard, P. L., and Kastelein, J. J. (2018) Inclisiran for the treatment of cardiovascular disease: The ORION clinical development program. *Future Cardiol.* **14**, 433–442
35. Seidah, N. G., Prat, A., Pirillo, A., Catapano, A. L., and Norata, G. D. (2019) Novel strategies to target proprotein convertase subtilisin kexin 9: Beyond monoclonal antibodies. *Cardiovasc. Res.* **115**, 510–518
36. Demina, E. P., Smutova, V., Pan, X., Fougerat, A., Guo, T., Zou, C., Chakraberty, R., Snarr, B. D., Shiao, T. C., Roy, R., Orekhov, A. N., Miyagi, T., Laffargue, M., Sheppard, D. C., Cairo, C. W., *et al.* (2021) Neuraminidases 1 and 3 trigger atherosclerosis by desialylating low-density lipoproteins and increasing their uptake by macrophages. *J. Am. Heart Assoc.* **10**, e018756
37. Thomas, G. (2002) Furin at the cutting edge: From protein traffic to embryogenesis and disease. *Nat. Rev. Mol. Cell Biol.* **3**, 753–766
38. [preprint] Gu, Y., Cao, J., Zhang, X., Gao, H., Wang, Y., Wang, J., Zhang, J., Shen, G., Jiang, X., Yang, J., Zheng, X., Xu, J., Zhang, C. C., Lan, F., Qu, D., *et al.* (2020) Interaction network of SARS-CoV-2 with host receptome through spike protein. *bioRxiv*. https://doi.org/10.1101/2020.09.09.287508
39. Morens, D. M., and Fauci, A. S. (2020) Emerging pandemic diseases: How we got to COVID-19. *Cell* **182**, 1077–1092
40. Zamorano Cuervo, N., and Grandvaux, N. (2020) ACE2: Evidence of role as entry receptor for SARS-CoV-2 and implications in comorbidities. *Elife* **9**, e61390
41. Mokhtari, T., Hassani, F., Ghaffari, N., Ebrahimi, B., Yarahmadi, A., and Hassanzadeh, G. (2020) COVID-19 and multiorgan failure: A narrative review on potential mechanisms. *J. Mol. Histol.* **51**, 613–628
42. Munzer, J. S., Basak, A., Zhong, M., Mamarbachi, A., Hamelin, J., Savaria, D., Lazure, C., Hendy, G. N., Benjannet, S., Chretien, M., and Seidah, N. G. (1997) *In vitro* characterization of the novel proprotein convertase PC7. *J. Biol. Chem.* **272**, 19672–19681
43. Ozden, S., Lucas-Hourani, M., Ceccaldi, P. E., Basak, A., Valentine, M., Benjannet, S., Hamelin, J., Jacob, Y., Mamchaoui, K., Mouly, V., Despres, P., Gessain, A., Butler-Browne, G., Chretien, M., Tangy, F., *et al.* (2008) Inhibition of chikungunya virus infection in cultured human muscle cells by furin inhibitors: Impairment of the maturation of the E2 surface glycoprotein. *J. Biol. Chem.* **283**, 21899–21908

44. Seidah, N. G., Mowla, S. J., Hamelin, J., Mamarbachi, A. M., Benjannet, S., Toure, B. B., Basak, A., Munzer, J. S., Marcinkiewicz, J., Zhong, M., Barale, J. C., Lazure, C., Murphy, R. A., Chretien, M., and Marcinkiewicz, M. (1999) Mammalian subtilisin/kexin isozyme SKI-1: A widely expressed proprotein convertase with a unique cleavage specificity and cellular localization. *Proc. Natl. Acad. Sci. U. S. A.* **96**, 1321–1326
45. Roubtsova, A., Munkonda, M. N., Awan, Z., Marcinkiewicz, J., Chamberland, A., Lazure, C., Cianflone, K., Seidah, N. G., and Prat, A. (2011) Circulating proprotein convertase subtilisin/kexin 9 (PCSK9) regulates VLDLR protein and triglyceride accumulation in visceral adipose tissue. *Arterioscler. Thromb. Vasc. Biol.* **31**, 785–791
46. Hassan, H. H., Bailey, D., Lee, D. Y., Iatan, I., Hafiane, A., Ruel, I., Krimbou, L., and Genest, J. (2008) Quantitative analysis of ABCA1-dependent compartmentalization and trafficking of apolipoprotein A-I: Implications for determining cellular kinetics of nascent high density lipoprotein biogenesis. *J. Biol. Chem.* **283**, 11164–11175